dI3 NEURONS MEDIATE SPINAL MOTOR LEARNING

Emam Khan

Thesis submitted to the University of Ottawa
in partial Fulfillment of the requirements for the
Master of Science in Biology

Department of Biology
Faculty of Science
University of Ottawa

Abstract

Motor learning, traditionally attributed to supraspinal structures, is increasingly recognized as a process that can occur within the spinal cord through intrinsic plasticity and circuit reorganization. Here, we investigate the role of a class of excitatory spinal interneurons—dorsal interneuron 3 (dI3)—in the acquisition of novel motor behaviors independent of supraspinal input. Using a real-time, closed-loop stimulation paradigm in spinalized mice, we promoted a persistent adaptation in the hindlimb position to be higher than its resting level by delivering saphenous nerve stimulation contingent on hindlimb position. The stimulation intensities were calibrated to selectively recruit low-threshold mechanoreceptors (LTMRs) that provide input to dI3s and mediate non-nociceptive sensory input relevant to motor control. To test the contribution of dI3s in this learning, inhibitory DREADD (hM4Di) receptors were expressed in $Isl1^{+}$/$VGLUT2^{+}$ cells, achieving reversible, cell-type-specific silencing of dI3s. Our results demonstrate that closed-loop stimulation reliably induces spinal motor learning, evidenced by a sustained behavioural change—elevation of hindlimb position above a preset vertical threshold. Chemogenetic silencing of dI3s abolished this motor learning at LTMR-selective stimulation intensities, and performance did not improve with repeated trials under dI3 inhibition. These findings indicate that dI3 activity is essential for the acquisition of new spinal motor skills with learning that is driven primarily by LTMR input. This work advances our understanding of the cellular and circuit mechanisms underlying spinal motor learning and highlights dI3s as a critical component of experience-dependent motor adaptation in the absence of supraspinal input.

Résumé

L'apprentissage moteur, traditionnellement attribué aux structures supraspinales, est de plus en plus reconnu comme un processus pouvant également se produire au sein de la moelle épinière grâce à la plasticité intrinsèque et à la réorganisation des circuits. Ici, nous examinons le rôle d'une classe d'interneurones excitateurs spinaux—les interneurones dorsaux de type 3 (dI3)—dans l'acquisition de nouveaux comportements moteurs indépendamment de l'apport supraspinal. À l'aide d'un paradigme de stimulation en boucle fermée en temps réel chez des souris spinalisées, nous avons favorisé une adaptation persistante de la position du membre postérieur afin qu'il demeure plus élevé que son niveau de repos, en administrant une stimulation du nerf saphène conditionnelle à la position du membre. Les intensités de stimulation étaient calibrées pour recruter sélectivement les mécanorécepteurs à seuil bas (LTMRs), qui transmettent des signaux sensoriels non-nociceptifs pertinents pour le contrôle moteur et fournissent des entrées aux dI3. Pour tester la contribution des dI3 dans cet apprentissage, des récepteurs DREADD inhibiteurs (hM4Di) ont été exprimés dans les cellules Isl1^{+}/VGLUT2^{+}, permettant une inhibition réversible et spécifique des dI3. Nos résultats démontrent que la stimulation en boucle fermée induit de façon fiable un apprentissage moteur spinal, comme en témoigne un changement comportemental soutenu—l'élévation du membre postérieur au-dessus d'un seuil vertical prédéfini. L'inhibition chimio-génétique des dI3 a aboli cet apprentissage moteur aux intensités de stimulation sélectives des LTMR, et la performance ne s'est pas améliorée lors de répétitions sous inhibition des dI3. Ces résultats indiquent que l'activité des dI3 est essentielle à l'acquisition de nouvelles habiletés motrices spinales, lorsque l'apprentissage est principalement guidé par l'apport des LTMR. Ce travail fait progresser notre compréhension des mécanismes cellulaires et des circuits sous-jacents à l'apprentissage moteur spinal et met en évidence le rôle critique des dI3 dans l'adaptation motrice dépendante de l'expérience en l'absence d'apport supraspinal.

Acknowledgements

I would like to express my deepest gratitude to my supervisor, Dr. Tuan Bui, for being the best mentor I could have asked for. His guidance, support, and unwavering belief in me shaped every step of this journey, and I feel incredibly fortunate to have learned under his leadership.

I am also profoundly grateful to my lab members—Dr. Sara Goltash, Dr. Lauren Couvrette, Dr. Alex Laliberte, Dr. Stephanie Gaudreau, Sarah Chiasson and Shahriar Nasari. Their brilliance, kindness, and sense of camaraderie made coming into the lab every day over the past two years an absolute joy. I couldn't have asked for a more inspiring group of people to work alongside.

I would like to thank the Animal Care and Veterinary Staff for their invaluable support, especially Julie Tremblay, who was with me every day to care for our animals and assist with my project. Her warmth, reliability, and genuine care meant a great deal to me throughout this experience.

I am sincerely grateful to my thesis advisory committee members, Dr. John Lewis and Dr. Simon Chen, for their thoughtful guidance and encouragement throughout this project. Their expertise and insight helped shape this work and challenged me to think more critically at every stage. I deeply appreciate their kindness, support, and the time they dedicated to helping me grow as a researcher.

I am also deeply thankful to Dr. Eve Tsai for funding my Master's and for being a constant source of inspiration. Her belief in me has been incredibly motivating, and I truly hope that the work we're doing at uOttawa will one day make a meaningful difference for patients.

Finally, I would like to thank my family for always believing in me, inspiring me, and supporting me unconditionally. Their love and encouragement have meant everything.

Statement of Contribution

Sarah Chiasson provided extensive training and support throughout this project. She taught me how to perform animal surgeries and properly care for the mice, and she assisted during many of my experiments. Dr. Sara Goltash played a critical role in the daily care of the animals and was an invaluable source of support throughout the project, helping me every day with animal monitoring and experimental logistics. Dr. Lauren Couvrette contributed to the project by assisting with animal surgeries and providing technical expertise during surgical procedures. Dr. Alex Laliberte was instrumental in teaching me surgical techniques and also performed many of the surgeries used in this study. Shahriar Nasari contributed to both the experimental work and the creation of figures, supporting data collection and visualization efforts.

Table of Contents

List of Figures

List of Abbreviations

dI3 – Dorsal Interneuron 3

DREADD – Designer Receptors Exclusively Activated by Designer Drugs
hM4Di – Human M4 muscarinic receptor (inhibitory DREADD)
J60 – JHU37160 (DREADD agonist)

GS – Gastrocnemius
TA – Tibialis anterior
SN – Saphenous nerve

AAV – Adeno-associated virus
CNS – Central nervous system
DAPI – 4′,6-diamidino-2-phenylindole
DLC – DeepLabCut
EMG – Electromyography
EPSC – Excitatory postsynaptic current
HRP – Horseradish peroxidase
Isl1 – ISL LIM Homeobox 1
LTMR – Low-threshold mechanoreceptor
MN – Motoneuron
OCT – Optimal cutting temperature compound
PBS – Phosphate-buffered saline
PFA – Paraformaldehyde
RFP – Red fluorescent protein
TTL – Transistor-transistor logic
vGluT2 – Vesicular glutamate transporter 2
µm – Micrometer

1.0 Introduction

1.1 Project overview

The central nervous system (CNS) integrates sensory input with motor output to generate movements. The CNS is able to acquire and retain motor skills following repetition in a process termed sensorimotor adaptation or "motor learning". Motor learning can be specifically defined as a set of internal processes associated with practice or experience that lead to improvements in the ability to produce goal-directed movements, often mediated by changes in neural circuits (Adams, 1971; Krakauer & Mazzoni, 2011; Schmidt & Lee, 2019; Shadmehr & Wise, 2004). Motor learning may involve multiple areas of the CNS that contain different specialized neural circuits underlying this process. Here, we focus on the spinal cord and explore the spinal circuitry that is involved in motor learning. We hypothesize that a specific class of spinal interneurons play an important role in the acquisition of new movements— dI3 neurons.

1.2 Spinal motor learning

1.2.1 Expanding the scope of motor learning

Motor learning has traditionally been attributed to supraspinal structures such as the motor cortex and cerebellum (Bastian et al., 1996; Criscimagna-Hemminger et al., 2010; Gibo et al., 2013; Morton & Bastian, 2006; Nguyen-Vu et al., 2013; Smith & Shadmehr, 2005; Synofzik et al., 2008; Taylor et al., 2010; Wolpert et al., 1998), yet accumulating evidence demonstrates that the spinal cord itself is also capable of supporting motor learning through circuit reorganization and intrinsic plasticity (de Leon et al., 1998; Grau et al., 2004; Kubasak et al., 2008; Lavaud et al., 2024; Lavrov et al., 2008; Leblond et al., 2003; Lovely et al., 1986; Rossignol & Frigon, 2011; Takeoka et al., 2014a; Wang et al., 2024; Wolpaw, 2007, 2010).

Motor learning in the brain is typically studied using complex tasks that involve multiple sensory modalities and goal-directed behavior. For example, reaching for an object while adapting to external perturbations engages proprioception, touch, vision, and cognitive components such as intention and error prediction (Bastian et al., 1996; Criscimagna-Hemminger et al., 2010; Gibo et al., 2013; Morton & Bastian, 2006; Nguyen-Vu et al., 2013; Smith & Shadmehr, 2005; Synofzik et al., 2008; Taylor et al., 2010; Wolpert et al., 1998). In contrast, motor learning within the spinal cord involves much simpler behaviors, such as reflexive hindlimb elevation driven by proprioceptive and cutaneous afferent feedback. These spinal processes do not involve volitional intent or supraspinal input. Because of this, spinal motor learning is often considered a form of motor adaptation rather than complex skill acquisition. In this thesis, we use the term spinal motor learning to describe this simpler, brain-independent form of adaptation.

1.2.2 Physiological and functional organization of the spinal cord

The spinal cord is a critical component of the central nervous system, serving as the primary communication pathway between the brain and the body. Structurally, it is organized into four major regions — cervical, thoracic, lumbar, and sacral — each giving rise to spinal nerves that innervate specific body segments. The spinal cord is responsible for a wide range of physiological functions, including the regulation of breathing, the coordination of locomotor activity through central pattern generators, and the mediation of reflexive responses (Bear et al., 2020; Grillner & El Manira, 2020; Kandel et al., 2021).

Experimental paradigms have shown that the spinal cord can encode and retain experience-dependent modifications in motor output, even in the complete absence of supraspinal input (Grau et al., 2004; Wolpaw, 2007, 2010). Importantly, spinal motor learning can be categorized into two

broad domains: (1) the relearning of a previously acquired motor behavior through spinal mechanisms alone (de Leon et al., 1998; Kubasak et al., 2008; Lavrov et al., 2008; Leblond et al., 2003; Lovely et al., 1986; Orsal et al., 2002; Rossignol & Frigon, 2011; Takeoka et al., 2014; Wang et al., 2024), and (2) the de novo learning of a novel motor behavior driven exclusively by spinal circuits (Buerger & Fennessy, 1971; Grau et al., 2004; Lavaud et al., 2024). These distinct forms of learning emphasize the spinal cord's capacity not only to adapt motor output to changing environmental and sensory demands but also to serve as an independent substrate for motor memory formation. This section first reviews the studies that have explored the role of the spinal cord in relearning previously acquired motor behaviors and studies investigating the acquisition of new motor skills, and concludes by outlining how this current study aims to advance the research of spinal motor learning of new skills.

1.2.2 Relearning Motor Behaviors After Spinal Cord Injury

Numerous studies have investigated the ability to relearn previously acquired motor behaviors through spinal mechanisms alone. One of the most extensively studied paradigms involves the recovery of locomotor function following complete transection (i.e. complete separation of the spinal cord from the brain). This area of research holds significant clinical relevance, particularly in efforts to restore walking ability after spinal cord injury. Using various animal models, researchers have assessed locomotor recovery over time and in response to different treatments. For example, both mice and cats have demonstrated the ability to regain hindlimb stepping following transection (Leblond et al., 2003; Martinez et al., 2012), while rats have shown similar improvements when training is paired with neurochemical stimulation (Orsal et al., 2002; Yakovleff et al., 1989). These findings demonstrate that functional recovery can occur

in the absence of supraspinal input, supporting the idea that motor behavior can be re-learned through plasticity within spinal circuits.

Several studies have explored the behavioural and physiological mechanisms underlying recovery after spinal cord injury, emphasizing the importance of training-induced plasticity. Repeated, task-specific locomotor training has been shown to significantly enhance stepping ability in animal models with complete lesions. In adult cats, treadmill training with partial weight support restored coordinated hindlimb stepping, marked by phase-dependent muscle activation and interlimb alternation (Lovely et al., 1986). Similar improvements were observed in neonatal rats, where repeated treadmill exposure after transection enhanced stepping patterns and modulated reflexes and circuit excitability (Kubasak et al., 2008). Physiologically, training led to increased excitability in flexor and extensor circuits, suggesting reorganization of central pattern generators below the lesion (Lavrov et al., 2008). Muscle spindle afferents have also been implicated in activity-dependent plasticity (Takeoka et al., 2014; Wang et al., 2024) showed that spinal motor learning induces shortening of the axon initial segment and lowers the firing threshold of spinal interneurons, indicating that plasticity involves both synaptic and cell-intrinsic mechanisms. Together, these findings highlight that recovery depends not just on spontaneous reorganization, but on repeated, sensory-driven engagement of motor circuits that reshape spinal physiology in a structured and meaningful way (de Leon et al., 1998; Rossignol & Frigon, 2011).

These studies illustrate an extreme case of motor recovery, in which the CNS is severely disrupted. However, these findings can also be viewed through a broader lens— as evidence of the spinal cord's capacity to modify motor behavior in response to changing demands. The ability to adapt motor output is fundamental to normal physiology. Because the environment is dynamic, motor behavior must be flexible: locomotion differs when walking on uneven surfaces, carrying a

heavy load, or navigating under adverse sensory conditions such as cold temperatures (Kent et al., 2019; Obeidat et al., 2023; Racinais & Oksa, 2010). These variations require ongoing adjustments in muscle activation patterns, coordination, and timing. The evidence suggests that spinal circuits may contribute to this continuous fine-tuning of motor output. Importantly, the CNS is unlikely to be pre-equipped with hardwired solutions for every possible environmental condition. Instead, it must acquire *new* motor strategies through interaction and repetition—suggesting that it does not merely adapt existing behaviors, but learns entirely new ones. This raises a key question: can the spinal cord participate in the learning of novel motor behaviors, rather than simply relearning those that were previously acquired?

1.2.3 De novo motor skill learning by the spinal cord

The spinal cord can indeed learn new motor skills, as shown initially by Buerger & Fennessy (1971), who demonstrated instrumental learning in spinalized rats. In this study, rats underwent complete spinal transection at the thoracic level, eliminating all supraspinal input. They had two separate groups: the learner rats and the control rats. The researchers then applied a shock-contingent learning paradigm: when the learner rat's hindlimb extended into an electrolyte solution, it received a mild shock; when the leg was flexed, no shock was delivered. The control rats receive the same number of shocks at the same time as the learner rats, but these were delivered independently of their limb position. The only difference between groups was that, for learners, shock delivery was contingent on hindlimb extension, whereas for controls, it was not. Over time, the learner rats maintained the limb in a flexed position to avoid the shock, despite having no input from the brain. Control rats failed to develop this behaviour. These findings provided some of the first evidence that the spinal cord can encode and retain new information through experience-

dependent mechanisms, establishing a precedent for spinal learning beyond reflex adaptation or re-learning of previously acquired tasks.

Lavaud et al. (2024) furthered this research, focusing specifically on molecularly-defined class of spinal neurons that are involved in motor learning: Ptf1a (pancreatic transcription factor 1a)-expressing cells, which includes dI4 neurons—inhibitory GABAergic interneurons in the spinal cord (Mona et al., 2020; Nishida et al., 2010) and Tlx3 (T cell leukemia homeobox 3)-expressing, which includes dI3 and dI5 neurons—excitatory glutamatergic interneurons in the spinal cord (Cheng et al., 2004; Guo et al., 2012; Kondo et al., 2008; Monteiro et al., 2021). Using a similar closed-loop conditioning paradigm where specific hindlimb of transected mice were electrically stimulated when the limb dropped below a vertical threshold, they showed that the learner group could learn to elevate their hindlimb above a threshold, where the control group could not. They went further to test different phases of motor learning: the acquisition and the recall of the behaviour. They repeated the learning trial multiple times in the same group of mice, measuring how many stimulations were required to induce hindlimb learning.

They found that both $Tlx3^+$ neurons and $Ptf1a^+$ neurons are critical for the acquisition of learned behavior. When these neurons were ablated, mice failed to associate foot position with aversive cues and did not adjust their motor output accordingly, despite preserving basic limb withdrawal responses. $Tlx3^+$ neurons are known to receive strong monosynaptic inputs from both proprioceptive and low-threshold cutaneous afferents and are also implicated to receive nociceptive inputs (Bui et al., 2013; Xu et al., 2008). This suggests that they are able to relay the electrical “instructive cues” used in the conditioning paradigm. Therefore, their data suggests that loss of $Tlx3^+$ activity disrupts the saliency or detection of these instructive stimuli, thereby preventing the formation of necessary association of sensory feedback with limb position. This

highlights Tlx3$^+$ neurons as a potential bottleneck for learning: if the teaching signal is degraded, the motor circuit cannot adapt.

1.2.4 Open questions and study rationale

Lavaud et al. (2024) raise several important questions about the mechanisms underlying spinal motor learning. While their study establishes that Tlx3$^+$ neurons are necessary for learning, it leaves open which specific subclasses within this lineage are responsible. Tlx3 marks a broad progenitor domain that gives rise to two types of excitatory glutamatergic interneurons in the dorsal spinal cord—dI3 and dI5 neurons (Guo et al., 2012; Kondo et al., 2008; Monteiro et al., 2021; Xu et al., 2008). One of our goals is to narrow this scope by focusing on dI3s, a well-characterized subclass within the Tlx3 lineage, to assess their specific contribution to spinal motor learning. This objective is based on the rationale that different subclasses likely serve specialized roles in sensory integration and motor adaptation.

A second unresolved aspect from the Lavaud study is whether only one type of instructive sensory input could induce learning. While previous studies—such as those by Buerger & Fennessy (1971) and Grau et al. (2004)—used clearly nociceptive stimuli, Lavaud et al. stimulated the hindlimb muscle at a fixed current which activated proprioceptive, Aβ, Aδ and C fibres as per their single unit electrophysiological recordings. Whether only the Aβ fibre could induce learning in their paradigm therefore remain unclear. We propose to build on this by stimulating more defined afferent populations—such as selectively targeting a cutaneous nerve in the hindlimb—and calibrating the stimulation intensity at threshold. If learning still occurs under these more specific conditions, we can infer that low-threshold mechanoreceptors (LTMRs), rather than nociceptors, are sufficient for learning. This would not only clarify whether this sensory modality

could alone induce learning but also determine whether dI3s are able to integrate cutaneous sensory input for motor learning.

Finally, we can examine short-term learning dynamics where multiple trials repeated within session with dI3 activity inhibition. It is possible that dI3 inhibition does not completely prevent motor learning, but instead increases the number of stimulations or time required for it to emerge beyond the limits of our 300-second trial. Repeating trials within a single session under dI3 inhibition can therefore reveal whether performance fails to improve or rapidly decays across repetitions—findings that would further support a role for dI3s in the acquisition of spinal motor learning.

Together, our study aims to further our understanding of the dorsal spinal interneurons involved in motor learning. Specifically, we seek to dissect the contribution of dI3 neurons in motor learning, identify the types of sensory input they integrate, and explore its role in the temporal aspect of motor learning.

1.3 dI3 neurons

dI3 neurons possess several characteristics that make them ideally suited to be involved in motor adaptation. In general, spinal neurons are organized into laminar structures that facilitate communication between peripheral inputs and central circuits within the spinal cord (Asan et al., 2022; Lai et al., 2016; Osseward & Pfaff, 2019; Rexed, 1952). Sensory afferents enter through the dorsal horn, motor (efferent) neurons project from the ventral horn, and interneurons occupy intermediate regions, forming complex microcircuits linking sensory inputs with motor commands (Bui et al., 2015; Harding et al., 2020; Rivera-Arconada et al., 2025; Todd, 2010, 2017). The interneurons serve as integrative hubs, shaping motor output by processing sensory input and

coordinating spinal reflexes and voluntary movements (Chad, 2003). Spinal interneurons may be excitatory or inhibitory, releasing neurotransmitters such as glutamate, GABA, or glycine (Brownstone & Bui, 2010; Bui et al., 2015). Interneuronal activity is essential for integrating sensory feedback, generating rhythmic motor patterns, coordinating muscle synergies, and relaying descending commands from supraspinal centers (Chapman et al., 2025; Dougherty et al., 2013; Kwan et al., 2009; Talpalar et al., 2013; Zhang et al., 2014).

Dorsal interneuron 3 (dI3) is a distinct class of spinal interneurons that are located primarily in the intermediate gray matter, specifically in laminae V–VII (Bui et al., 2013). They are excitatory glutamatergic and are crucial for integrating sensory and motor signals (Bui et al., 2013, 2016; Goltash et al., 2023). dI3s receive strong monosynaptic inputs from both proprioceptive and low-threshold cutaneous afferents, enabling them to directly process sensory information (Bui et al., 2013). Polysynaptic EPSCs were also observed when sensory afferents were stimulated at magnitudes strong enough to recruit nociceptive afferents, suggesting that they may integrate nociceptive signals conveyed by other spinal neurons (Bui et al., 2013).

dI3s are identified by their expression of two key markers. Firstly, ISL LIM Homeobox 1 (Isl1) is a LIM-homeodomain transcription factor that is shared amongst cholinergic spinal motoneurons and sensory neurons of the dorsal root ganglia but is exclusively expressed in dI3s within the intermediate spinal cord (Alaynick et al., 2011; Bui et al., 2013, 2016; Liem et al., 1997). Secondly, Vesicular glutamate transporter 2 (vGluT2), which is responsible for packaging glutamate into synaptic vesicles, is expressed in the vast majority of dI3s (Bui et al., 2013; Goltash et al., 2023; Li et al., 2020; Papathanou et al., 2018). These markers allow us to target dI3s to disrupt their activity.

dI3s are involved in a wide array of motor behaviors, including hand grasping and locomotion (Bui et al., 2013, 2016; Nasiri et al., 2024). They project to motoneurons and are capable of activating locomotor networks (Bui et al., 2016; Goltash et al., 2023; Nasiri et al., 2024). Optogenetic stimulation of dI3s in the lumbar spinal cord can independently recruit rhythmic locomotor activity, suggesting their involvement in generating and coordinating locomotion. Moreover, these neurons are essential for the recovery of locomotor activity following spinal cord injury, as inhibiting their activity impairs locomotor recovery in spinal transected mice, compared to controls with unaltered dI3 activity (Bui et al., 2016).

1.4 Hypothesis

It is hypothesized that dI3 activity is required for spinal motor learning of new skills. dI3s have been previously shown to mediate locomotor recovery after spinal transection (Bui et al., 2016), suggesting their capacity to integrate sensory signals in adaptive motor processes. Additionally, Lavaud et al. (2024) showed that $Tlx3^{+}$ neurons, which give rise to dI3s, are required for motor learning. Based on this, we predict that disruption of neural activity of dI3s will impair the spinal cord's ability to acquire new motor behaviors.

1.5 Objectives

1) Determine whether dI3 neurons are required for spinal motor learning, and to identify which behavioral parameters—such as the number of stimulations required for learning or the height of limb elevation—are affected by the disruption of dI3 activity.

2) Determine whether the activation of low-threshold mechanoreceptors (LTMRs) alone is sufficient to drive spinal motor learning, in the absence of nociceptive input. Assess whether dI3 neurons play a role in spinal motor learning mediated by different types of sensory inputs.
3) Assess the effects of repeated closed-loop trials within a single session under dI3 inhibition to determine whether performance fails to improve or rapidly declines across repetitions, which would provide further evidence that dI3s contribute to the acquisition of spinal motor learning.

2.0 Materials and Methods

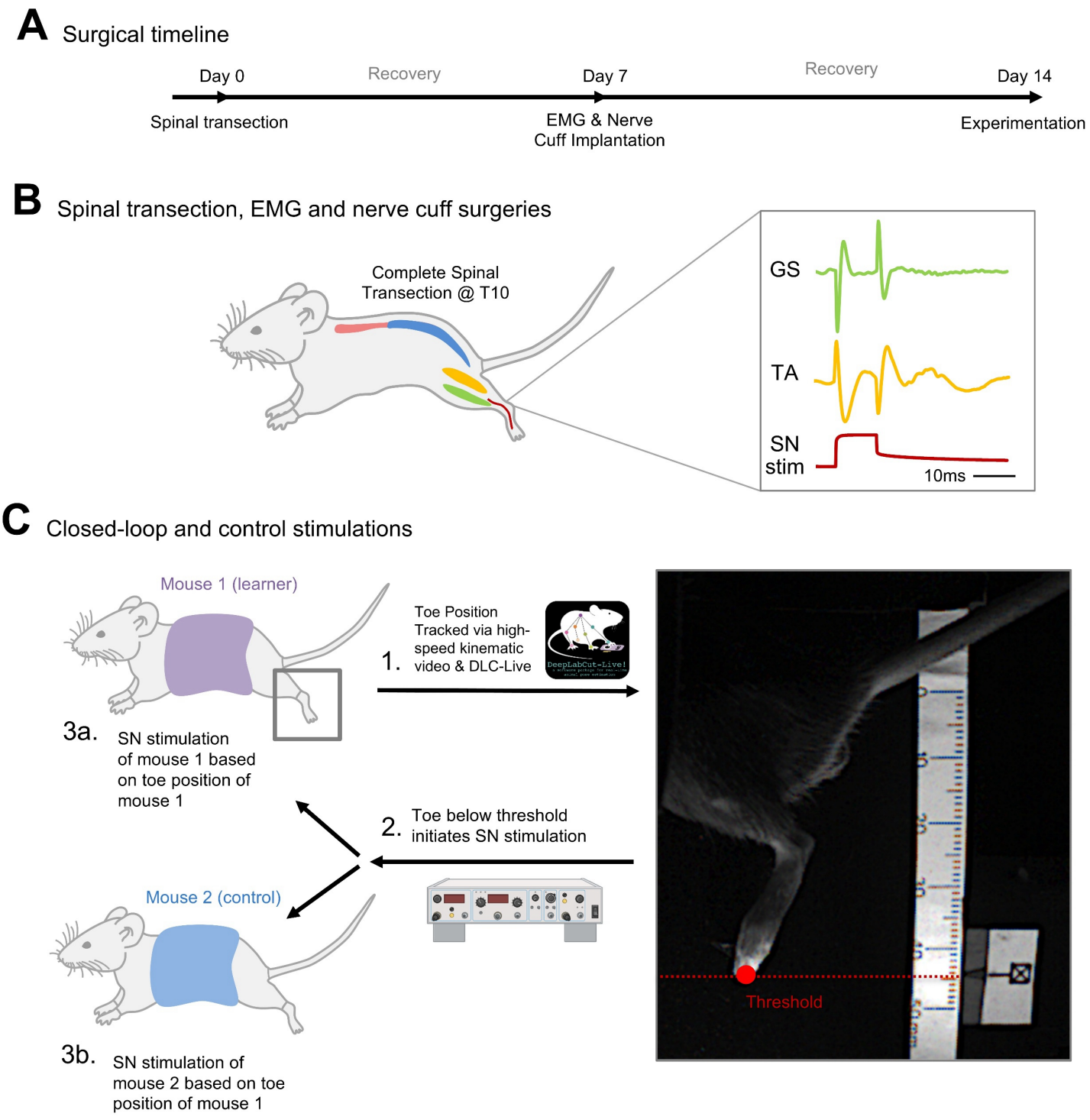

Figure 1: Experimental timeline, surgical procedures, and closed-loop stimulation paradigm. ***A,*** Schematic of the experimental timeline. Mice underwent complete spinal transection at approximately thoracic level T10 on Day 0. On Day 7, lateral gastrocnemius (GS) and tibialis anterior (TA) EMG electrodes were implanted and a saphenous nerve (SN) cuff was implanted. ***B,*** Illustration of surgical procedures, including spinal transection and implantation of EMG electrodes and nerve cuff. Representative EMG traces from GS and TA muscles, along with the SN stimulation waveform, are shown. ***C,*** Diagram of the closed-loop and control stimulation paradigms.

2.1 Animals

All animal procedures were approved by the University of Ottawa Animal Care Committee and adhered to the guidelines established by the Canadian Council on Animal Care. Two genetically defined groups of mice were used to express hM4Di in targeted neuronal populations. The first group consisted of a transgenic line with the genotype Isl1-Cre x Vglut2-Flp x CreON-FlpON-hM4Di, resulting in hM4Di expression in Isl1+ and Vglut2+ cells through Cre/Flp-mediated recombination. Specifically, a RC::FPDi (CreON-FlpON-hM4Di) line was bred to a Isl1-Cre; Vglut2-Flp line to yield triple transgenic the Isl1/Vglut2-hM4Di line. The second group consisted of Isl1-Cre x Vglut2-Flp x CreON-FlpON-tdTomato mice that received spinal injections of an AAV vector carrying a Cre/Flp-dependent hM4Di-mCherry payload, allowing for targeted hM4Di expression using the same recombination strategy. Both groups are illustrated in Figure 2A (panels i and ii). All mice were obtained from The Jackson Laboratory.

A total of 8 adult mice (4 males and 4 females) were used in this study, ranging from 1–3 months of age at the time of initial surgery to 2–4 months by the end of behavioral testing. Mice were housed singly in individually ventilated cages under a 12:12 hour light/dark cycle (lights on from 7:00 a.m. to 7:00 p.m.), with room temperature and controlled humidity. Food (kibble), water, and supplemental diet gel were provided ad libitum. All testing was conducted between 8:00 a.m. and 8:00 p.m.

To ensure animal welfare, all mice underwent regular health monitoring following spinal cord transection. Bladder expressions were performed as needed, and comprehensive health checks—including assessments of activity, hydration, fur coat, urine, eyes, breathing, and overall condition—were conducted three times daily. Veterinary support was always available, with direct

contact maintained with University of Ottawa veterinarians for any signs of animal distress or discomfort.

2.2 Expression of hM4Di receptors

To temporarily inhibit the activity of dI3s, we expressed the inhibitory Designer Receptor Exclusively Activated by Designer Drugs (DREADD) receptor hM4Di in Isl1^{+}/VGLUT2^{+} cells. Mice were assigned to one of two experimental groups based on the method of receptor expression: a transgenic hM4Di group (n = 4) and an AAV-hM4Di group (n = 4).

In the transgenic hM4Di group (Fig. 2Ai), the hM4Di gene was inserted into the genome under the control of the CAG promoter. Its expression was blocked by loxP- and FRT-flanked STOP cassettes, which were only excised in cells co-expressing Cre (from the Isl1 promoter) and FlpO (from the VGLUT2 promoter), thereby restricting hM4Di expression to Isl1^{+}/VGLUT2^{+} cells —dI3s and a subset of sensory afferents involved in mechanical nociception (Lagerström et al., 2010).

In the AAV-hM4Di group (Fig. 2Aii), mice received six bilateral injections of an AAV2/8 vector (adeno-associated virus serotype 2 genome packaged in a serotype 8 capsid) carrying the hM4Di-mCherry gene under the control of the human synapsin (hSyn) promoter. As in the transgenic group, expression was limited to Isl1^{+}/VGLUT2^{+} cells by loxP- and FRT-flanked STOP cassettes placed upstream of the hM4Di gene. The mice received intraspinal injections of AAV at five weeks of age. One hour prior to surgery, mice were administered buprenorphine HCl (0.1 mg/kg, subcutaneously) for preoperative analgesia. Anesthesia was induced and maintained with isoflurane throughout the procedure. Mice were positioned in a stereotaxic frame, and a micro-

injector was used to deliver 0.3 µL of viral solution at each of three injection sites on both the right and left sides, targeting the laminar spaces between the T11, T12, T13, and L1 vertebral segments. This resulted in a total of six injections per animal, corresponding to the L2–L4 spinal cord segments. Postoperatively, mice received buprenorphine (0.1 mg/kg, Ceva Animal Health) for two days to manage pain. In addition, antibiotics (Baytril, Elanco) were provided in the drinking water for seven days to prevent infection. Mice were allowed to recover for at least one month prior to undergoing spinal cord transection surgery.

To activate hM4Di receptors, mice received a subcutaneous injection of 0.5 mg/kg of the designer drug JHU37160 (J60), which induces membrane hyperpolarization in hM4Di-expressing cells (Roth, 2016). The same dosage was used for saline control injections. A 15-minute waiting period following J60 administration to allowed for receptor activation, and all behavioral testing was completed within one hour—the estimated duration of drug activity (Benevides et al., 2025; Lawson et al., 2023; Singer et al., 2022). A washout period of 36 hours was allowed between J60 trials to ensure drug clearance prior to subsequent experiments.

2.3 Immunohistochemical detection of hM4Di expression in Isl1$^+$/VGLUT2$^+$ cells

Spinal cords were collected from AAV-hM4Di mice (n = 4) and transgenic hM4Di mice (n = 4). All mice were between 4-6 months old, with 4 males and 4 females. Following dissection, each cord was fixed by immersion in 5 mL of 4% paraformaldehyde (PFA) for 16 hours at 4°C. After fixation, tissues were transferred to a 30% sucrose solution in PBS for cryoprotection, then embedded in OCT compound and stored at –80°C until sectioning. Cervical and lumbar segments

of the spinal cord were sectioned at a thickness of 25 μm using a cryostat, and sections were stored at –4°C until staining.

For immunohistochemistry, sections were mounted onto standard glass slides and rinsed in PBS. Blocking was performed using 5% goat serum in PBS for 30 minutes at room temperature. To enhance detection of hM4Di-mCherry, sections were incubated with a rabbit polyclonal anti-RFP antibody (Rockland, 600-401-379-RTU; 1:500 dilution) for 48 hours at 4°C. After washing, sections were incubated with a goat anti-rabbit HRP-conjugated secondary antibody (Abcam, ab7090; 1:2000 dilution) for 3 hours at room temperature. Signal amplification was achieved using tyramide signal amplification (TSA) with 690 Opal dye (1:150 dilution in TSA buffer) for 8 minutes, followed by several washes in PBS. Nuclei were counterstained with DAPI (1:500 dilution) for 3 hours, included during secondary antibody incubation. No additional antibodies were used for Isl1 or VGLUT2 labeling, and no negative or isotype controls were included.

After staining, sections were coverslipped with Immunomount. Confocal imaging was performed using an Olympus FV1000 BX61 LSM microscope. DAPI was visualized using standard excitation/emission settings (excitation ~358 nm, emission ~461 nm), and hM4Di expression was detected using the far-red channel for the 690 Opal dye (excitation ~676 nm, emission ~694 nm). Images were processed and analyzed using ImageJ software, with adjustments to brightness and contrast and overlays of DAPI and hM4Di-mCherry channels. For Figure 1, representative images from one mouse are shown, although sections from 8 mice (4 males and 4 females) were analyzed in total.

2.4 Spinal cord transection surgical procedure

Mice were anesthetized with 2% isoflurane and placed in a prone position on a heating pad to maintain body temperature throughout the procedure. The skin was incised parallel to the body along the midline of the back, extending from the end of the cervical region to the end of the thoracic region, using fine surgical scissors. The underlying fascia was carefully removed with surgical forceps, and the muscle attached to the lamina at the thoracic level was dissected away bilaterally from the lamina.

To expose the T10 level of the spinal cord, the T7 and T8 laminae were cut on both sides with surgical scissors, accounting for the anatomical offset between spinal cord segments and vertebral levels. Two cuts were made at the T10 level, and the spinal cord segment was removed. Hemostasis was achieved by applying sterile surgical cotton swabs to absorb blood for approximately five minutes. Complete transection was ensured by using a surgical hook to gently scrape horizontally along the spinal column, severing any remaining tissue bridges. The area was again blotted for an additional five minutes until bleeding subsided.

The completeness of the transection was first confirmed intraoperatively by visual inspection, with particular attention to the lateral aspects of the column to ensure no residual connections remained. Post-mortem verification was also performed for all mice to confirm full transection.

Once the lesion site was confirmed, sterile surgical foam (Surgifoam, Johnson & Johnson Medtech) was placed in the cavity to prevent axonal regeneration across the lesion. The overlying muscle was closed using continuous 6-0 vicryl sutures (Ethicon), and the skin was closed with wound clips, which were removed one week later.

Preoperative analgesia included an injection of bupivacaine at a standard dose. Postoperative pain management consisted of subcutaneous buprenorphine (0.1 mg/kg, Ceva Animal Health) administered for three days. Carprofen was also administered post-operatively. The animals' body temperature and breathing rate were monitored throughout the procedure. Mice were individually housed in cages placed on a heating pad for the first two days after surgery and then returned to their standard housing conditions. Mice were allowed to recover for at least one week prior to behavioral testing. This surgical protocol was adapted in part from Goltash et al. (2025).

2.5 Fabrication of EMG muscle electrodes and nerve cuffs

Custom electromyography (EMG) muscle electrodes and nerve cuffs were fabricated using established protocols and commercially available materials and following the protocols described in previous mouse studies (Akay et al., 2006; Mayer & Akay, 2018; Pearson et al., 2005).

2.5.1 EMG Muscle Electrodes

Paired-wire bipolar EMG electrodes were constructed from 7-strand stainless steel wire (A-M Systems, cat. no. 793200; bare diameter 0.001", coated diameter 0.0055"). Each electrode was cut to a length of 7 cm from the connector to the needle. The wires were stripped of insulation, twisted together, and knotted at the midpoint to form the recording site. A 27G needle was attached to one end of the electrode pair to facilitate insertion into muscle tissue, while the opposite ends were soldered to gold pins (DigiKey, part no. SAM1155-08-ND) for connection to the headpiece.

2.5.2 Nerve Cuff Electrodes

Nerve cuffs were fabricated using paired stainless steel wires prepared as above. One end of the wires was threaded through a segment of silicone tubing (Alliedsil; internal diameter 0.020", outer diameter 0.037"), which served as the cuff. The cuff was designed to be placed around the saphenous nerve and secured with a silk suture passed through the silicone.

2.5.3 Connector Assembly

Both muscle and nerve cuff electrodes were connected to a central connector (DigiKey, part no. SAM15648-ND; length 10 mm), which was inserted subcutaneously in the back of the mouse at the thoracic region. The plastic housing of the connector was coated in a thin layer of biocompatible 5-Minute Epoxy Gel (Devcon) to ensure a smooth, rounded finish and minimize tissue irritation. The epoxy was allowed to cure for at least 24 hours prior to use.

2.5.4 Sterilization and Testing

All electrode assemblies were sterilized by immersion in 3% hydrogen peroxide for 25 minutes, followed by thorough rinsing with sterile distilled water immediately before implantation. Electrodes were tested for continuity and impedance before use to ensure proper function.

2.6 EMG and nerve cuff implantation surgeries

Surgical implantation of EMG muscle electrodes and nerve cuff electrodes was performed on all eight mice (Figs. 1B, 1C). For preoperative analgesia, mice received buprenorphine HCl

(0.1 mg/kg, subcutaneously) one hour prior to surgery. Anesthesia was induced and maintained with isoflurane throughout the procedure.

Two bipolar EMG electrodes were implanted per mouse, targeting the ankle flexor (tibialis anterior, TA) and extensor (gastrocnemius, GS) muscles of the left hindlimb. Additionally, a nerve cuff electrode was placed around the saphenous nerve (SN) of the left hindlimb. The surgical procedures for electrode implantation followed established protocols for hindlimb EMG recordings in mice (Akay, 2014; Akay et al., 2006).

Incisions were made in the upper neck region, hip, and over the hindlimbs to expose the target muscles and the saphenous nerve. Electrode wires were threaded subcutaneously from the neck incision through the hip incision and down to the hindlimb, then inserted into the muscle tissue parallel to the muscle fibers. The nerve cuff electrode was positioned around the saphenous nerve to enable electrical stimulation of cutaneous afferent fibers supplying the anterior distal hindlimb.

A connector was secured subcutaneously in the dorsal thoracic region using 5-0 Prolene sutures, with four interrupted knots anchoring the connector at each corner. All incisions were closed using 7-0 Prolene sutures (same brand as used in transection surgeries), employing an interrupted suture technique with multiple double knots per suture. Each hindlimb incision received 5–6 knots, and the hip incision was similarly closed after feeding the wires through. Postoperative analgesia included buprenorphine (0.1 mg/kg, subcutaneously) administered 6 hours after surgery and then every 12 hours for 48 hours. A topical application of bupivacaine (standard clinical concentration) was applied to all incisions at the time of surgery and at each analgesic time point to minimize irritation. For infection prophylaxis, a broad-spectrum antibiotic (Baytril, Elanco) was provided ad libitum in the drinking water for one-week post-surgery.

Mice were individually housed in cages placed on a heating pad for the first two days after surgery and then returned to their standard housing conditions. All animals were given at least one week to recover before beginning any acclimation or behavioral testing.

2.7 EMG recording and nerve stimulation

Muscle activity was recorded using a Differential AC Amplifier (A-M Systems, Model 1700) set to a gain of ×1000, with a low cut-off frequency of 300 Hz, a high cut-off frequency of 500 Hz, and the notch filter engaged. Signals were digitized using a Digidata 1440a system (Axon CNS, Molecular Devices) at a sampling rate of 10,000 Hz. Data were acquired using AxoScope software and analyzed with custom Python scripts and GraphPad Prism.

Electrical stimulation of the saphenous nerve was performed using a GRASS S88 Stimulator connected to a photoelectric stimulus isolation unit delivering constant current output. The polarity was set to normal, with a current range of 0.1–1.5 mA. Stimulation parameters included a pulse duration of 9 ms and current amplitudes of 0.3, 0.6, or 1.2 mA, set by adjusting the stimulator voltage and confirmed with a multimeter at the isolator output. A 1-second interval was maintained between pulses.

At the start of experimentation for each mouse, the stimulation threshold was empirically determined to ensure reliable, selective activation of Aβ sensory fibers, while minimizing recruitment of higher-threshold nociceptive afferents. Threshold was operationally defined as the minimum current amplitude required to elicit a clear, reproducible behavioral reflex—specifically, visible hindlimb withdrawal or muscle twitch—following a single electrical pulse. This behavioral

response was verified in real time by visual inspection of the limb and corroborated by detection of corresponding EMG activity in the target muscle.

To determine this threshold, stimulation pulses were delivered at gradually increasing current amplitudes starting from below anticipated threshold while keeping pulse duration, interval, and all other stimulation parameters identical to those later used in the experiment. For each candidate threshold, the response was tested at least ten times in succession to ascertain the frequency and consistency of the reflex. The current at which a reflex was reliably evoked in all trials (≥10/10 responses) was adopted as the animal's stimulation threshold. Across all mice tested, a current amplitude of 0.3 mA consistently elicited the threshold behavioral response and was thus used for all subsequent closed-loop trials. Threshold determinations were not blinded to animal or treatment. They were determined following saline injection, to ensure standardized and reproducible stimulation conditions across the study.

2.8 Closed-loop spinal motor learning paradigm

To investigate spinal motor learning, we implemented a closed-loop feedback system in which electrical stimulation of the SN was delivered contingent on the real-time position of the mouse’s toe (Fig. 1C). Each mouse was placed in a custom-made cardboard harness with a Velcro strap, individually fitted to ensure security without restricting respiration. The harness was suspended above the ground using a repurposed horizontal steel arm, allowing the left hindlimb to move freely. The mouse’s torso was held horizontal, with the tail taped above the camera’s field of view. To reduce stress and movement, the mouse’s front paws rested on a large tube positioned in front of the animal.

High-speed video was captured using a BASLER acA640-750µm camera (100 frames per second, 640×480 pixels), positioned directly in front of the left hindlimb. The right hindpaw was masked with black velvet tape to prevent mis-tracking, and black velvet paper was used as a backdrop to enhance contrast. Three LED lights illuminated the hindlimb for optimal video clarity. Video acquisition and real-time pose estimation were performed using a custom Python script built on DeepLabCut-Live! version 1.0.2, which directly controlled the camera. The neural network was trained on 800 manually labeled frames from practice session videos. DeepLabCut-Live pose estimation inferences of toe and threshold vertical positions were performed on an Intel Core i9-13900K CPU and RTX 4070TI GPU, achieving 10–20 ms per frame.

After harnessing, each mouse was acclimated for 10 minutes to allow the hindlimb to settle into its natural resting position. A ruler visible in the camera's field of view enabled spatial calibration. The script tracked both the toe and a physical "X" marker, which represented the vertical threshold, using DeepLabCut-Live. The vertical threshold was set approximately 2 mm above the resting toe position and could be adjusted manually by turning a knob that moved the "X" marker.

When the tracked toe dropped below the threshold, the Python script instructed a microcontroller (Arduino UNO, ELEGOO UNO R3) to send a TTL pulse. This pulse was routed through a custom "TTL to contact closure" converter, which triggered the GRASS S88 stimulator to deliver a stimulation pulse to the SN. The measured latency from threshold crossing to stimulation delivery was 10–20 ms. To ensure accurate triggering and minimize false positives, the script displayed the video feed and tracking confidence in real time, only allowing stimulation when DeepLabCut-Live's confidence exceeded 90%. A 1-second grace period was enforced between stimulations to limit frequency.

For each experiment, two mice were used: a learner and a control. The learner mouse received SN stimulation contingent on its own toe crossing the threshold (closed-loop), while the control mouse received SN stimulation at the exact same times, but independent of its own movements (open-loop/yoked control). Both mice were harnessed and positioned identically but placed on separate desks.

All experimental data—including video, estimated toe-to-threshold distances, tracked positions, and tracking confidence—were recorded by the custom Python script. Data analysis was performed using GraphPad Prism.

2.9 Analysis of electromyography (EMG) data

EMG activity from the gastrocnemius (GS) and tibialis anterior (TA) muscles was used to quantify muscle activation during behavioral trials. For the purpose of extracting muscle activation events and estimating overall muscle use, custom analysis routines were implemented to compute the signal envelope and to manually annotate bouts of activity.

First, a root-mean-square (RMS) envelope of the EMG signal was calculated using a continuous moving window with a duration of 20 ms. This step produced a smoothed representation of muscle activation amplitude across time and was used to visually assess the occurrence and timing of muscle activity events.

Manual annotation was performed using a custom-built Python script that enabled offline visualization and scrubbing of the RMS signal. Events were manually marked using a cursor interface. All annotations were performed blind to both animal identity and treatment condition (e.g., saline vs. J60). Annotations for both GS and TA muscles were curated independently. This manual approach was selected due to variability in signal amplitudes across individual animals—

largely stemming from slight inconsistency of signal transduction quality and the presence of electrical stimulation artifacts caused by saphenous nerve stimulation. These artifacts were qualitatively distinguishable from genuine muscle activity and excluded from analysis. The absence of a standardized quantitative thresholding method was thus intentional, allowing reliable distinguishing of true muscle events across animals despite variability in baseline signal-to-noise levels.

Muscle activity events were defined as transient increases in EMG amplitude (as visualized in the RMS envelope) that clearly exceeded the background level. Valid events typically ranged from 50 to 200 ms in duration and were only annotated if consistent with muscle-generated activity patterns rather than stimulation-induced artifacts. For each 5-minute behavioral trial, two outcome measures were computed per muscle: total number of discrete muscle activity events, and cumulative duration (sum of annotated event durations) of muscle activity.

These two metrics were computed independently for GS and TA muscles. For each animal, results were averaged across all available trials under each treatment condition (saline or J60), yielding a per-animal mean for each metric and condition. These values were then used for subsequent group-level comparisons.

3.0 Results

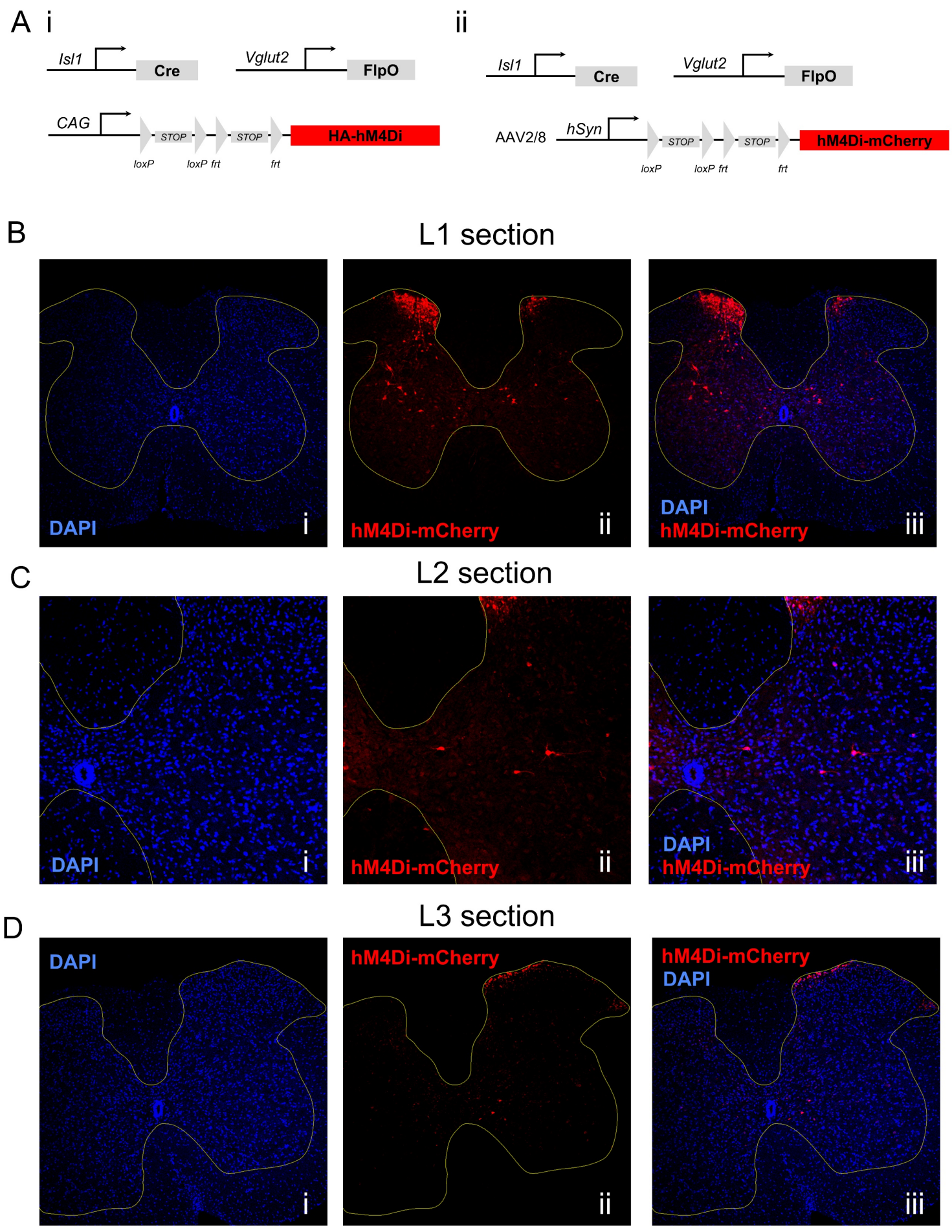
A i
Isl1
Cre
Vglut2
FlpO
CAG
STOP
STOP
HA-hM4Di
loxP
loxP frt
frt
ii
Isl1
Cre
Vglut2
FlpO
AAV2/8
hSyn
STOP
STOP
hM4Di-mCherry
loxP
loxP frt
frt
B
L1 section
DAPI
i
hM4Di-mCherry
ii
DAPI
hM4Di-mCherry
iii
C
L2 section
DAPI
i
hM4Di-mCherry
ii
DAPI
hM4Di-mCherry
iii
D
L3 section
DAPI
i
hM4Di-mCherry
ii
hM4Di-mCherry
DAPI
iii

Figure 2: Dual-recombinase-dependent expression of hM4Di-mCherry in lumbar spinal cord using transgenic and AAV-mediated strategies. ***A,*** Schematic of genetic strategies for targeting hM4Di expression to VGLUT2^{+}/Isl1^{+} cells. ***i,*** In the transgenic hM4Di group, the hM4Di gene is inserted into the genome under the control of the CAG promoter, but its expression is prevented by loxP- and FRT-flanked STOP cassettes. ***ii,*** In the AAV-hM4Di group, mice receive an AAV2/8 vector (adeno-associated virus serotype 2 genome packaged in a serotype 8 capsid) carrying the hM4Di-mCherry gene under the hSyn promoter (human synapsin promoter). ***B–D,*** Immunofluorescence images of lumbar spinal cord sections (L1, L2, L3) from a representative AAV-hM4Di mouse. For each section: (i) DAPI nuclear staining (blue), (ii) hM4Di-mCherry expression (red), and (iii) merged images. Yellow outlines indicate gray matter boundaries.

3.1 hM4Di expression in dI3s confirmed by immunohistochemistry

Figure 2 shows immunofluorescence images of lumbar spinal cord sections (L1, L2, L3) from a representative AAV-hM4Di mouse. hM4Di-mCherry–positive cells are observed in both the superficial dorsal horn (laminae I–II) and the deeper dorsal/intermediate laminae (laminae V–VII). Although we did not directly label dI3s, previous work has demonstrated that they are located predominantly in laminae V–VII of the lumbar spinal cord (Bui et al., 2013). Based on this, the hM4Di-mCherry–positive cells present in these laminae are likely to correspond to dI3s.

In addition, a subset of sensory afferents involved in mechanical nociception also express Isl1 and VGLUT2 (Lagerström et al., 2010). Afferents mediating mechanical nociception, including Aδ and C fibers, are known to terminate primarily in the superficial dorsal horn, specifically within laminae I–II (Armstrong & Herr, 2025; Light & Perl, 1979; Pan & Pan, 2004; Todd, 2017). Therefore, the hM4Di-mCherry–positive signal observed in laminae I–II likely represents the terminations of these nociceptive afferents.

The saphenous nerve contains Aβ, Aδ, and C fibers (Abraira & Ginty, 2013; Milenkovic et al., 2008). Aβ fibers are predominantly low-threshold mechanoreceptors (LTMRs) responsive to light touch, while Aδ and C fibers are primarily nociceptors (Abraira & Ginty, 2013). dI3s have been shown to receive direct input from LTMRs (Bui et al., 2013). Given that our objective is to determine the role of dI3s in motor learning using a closed-loop stimulation paradigm with saphenous nerve stimulation, it is important to note that hM4Di expression in Aδ and C fibers means these nociceptive afferents will also be hyperpolarized upon hM4Di activation. If the goal

is to isolate the function of dI3s, careful control of stimulation parameters is required to avoid confounding activation of nociceptive fibers, which could engage alternative circuitry.

To address this, we controlled the intensity of saphenous nerve stimulation. A previous study in rats has shown that the activation threshold for C fibers is approximately 4 times higher, and for Aδ fibers approximately 2.5 times higher, than that of Aβ fibers (Koga et al., 2005). Using our saphenous nerve cuff, we determined the behavioral threshold to be 0.3 mA. Accordingly, we conducted closed-loop stimulation trials at 0.3 mA to selectively activate Aβ fibers. To serve as experimental controls and to assess the effects of broader afferent recruitment, we also performed trials at 0.6 mA and 1.2 mA, which approximate the activation thresholds for Aδ and C fibers, respectively. This approach allowed us to distinguish the specific contributions of low-threshold mechanoreceptors from those of nociceptive afferents in our behavioral paradigm, and to control for potential confounding effects arising from the activation of pain pathways.

Saline | Closed-loop stimulation | 1.2 mA

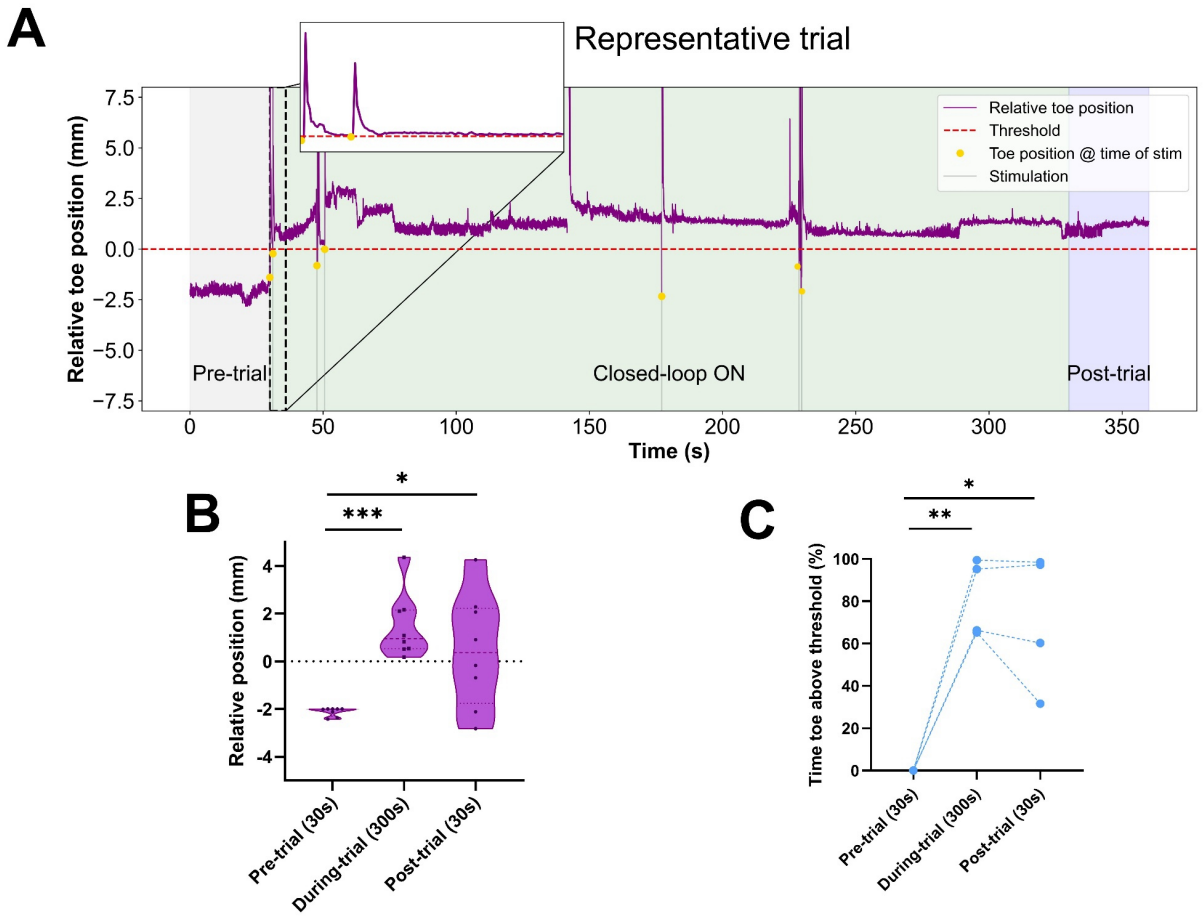

Saline | Control stimulation | 1.2 mA

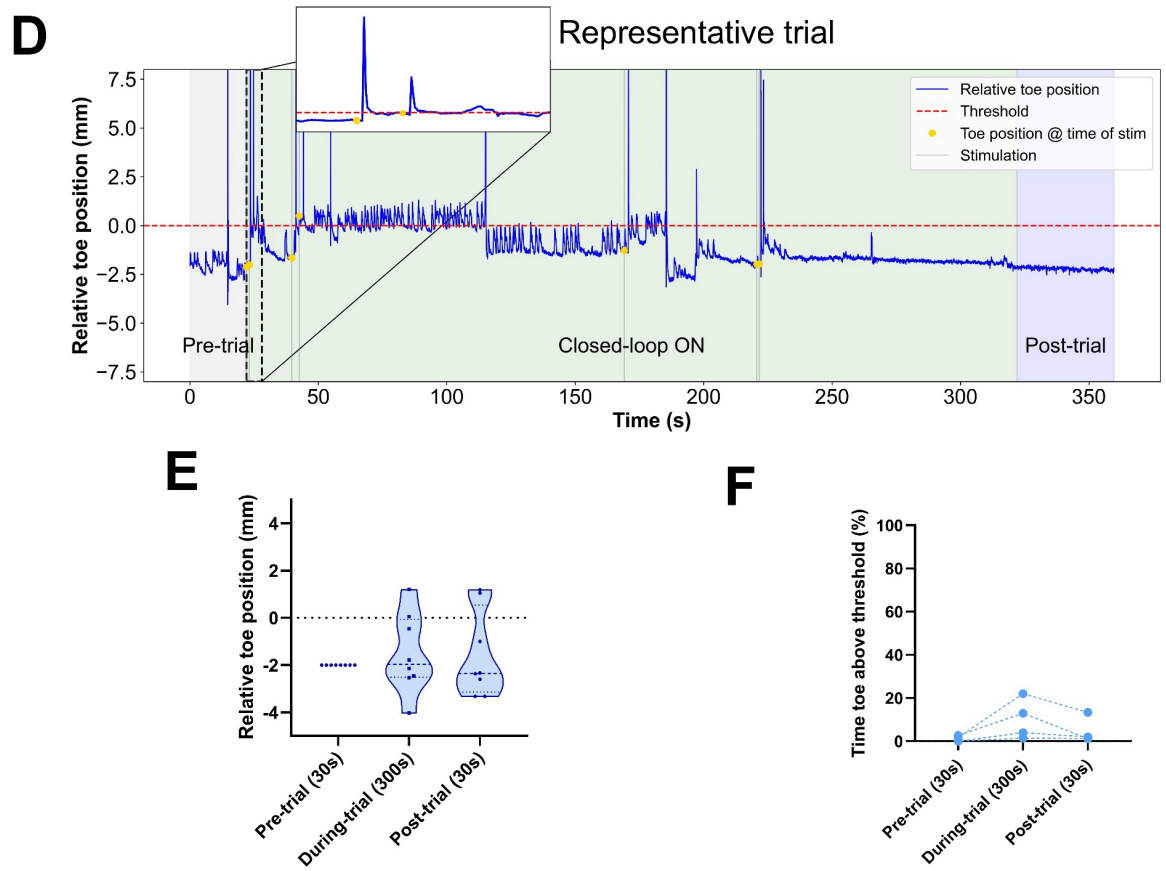

Figure 3: Closed-loop and control trials at 1.2 mA stimulations with saline administration. ***A,*** Representative trace of toe position during a closed-loop stimulation trial (saline administration with 1.2 mA stimulations). Stimulation times are indicated by vertical gray lines, with yellow dots marking toe position at the moment of stimulation. ***B,*** Average toe vertical position across trial phases in closed-loop stimulation trials (saline, 1.2 mA). Each point represents the mean value for a single animal, averaged across multiple trials ($n = 8$). *Comparisons,* pre-trial versus during-trial, $p = 0.0004$; pre-trial versus post-trial, $p = 0.0427$; during-trial versus post-trial, $p = 0.2061$. ***C,*** Proportion of time the toe remained above threshold during each trial phase with saline and 1.2 mA stimulations. Each point represents the mean value for a single animal, averaged across multiple trials ($n = 4$). Each line connects the mean values from the same subject. *Comparisons,* pre-trial versus during-trial, $p = 0.0061$; pre-trial versus post-trial, $p = 0.0419$; during-trial versus post-trial, $p = 0.5382$. ***D,*** Control stimulation trial paired with the trial shown in panel A. The same stimulation times were delivered to this subject, but independently of toe position, administered with saline. ***E,*** Average toe vertical position across trial phases in control stimulation trials (saline, 1.2 mA; $n = 8$). *Comparisons,* pre-trial versus during-trial, $p = 0.7057$; pre-trial versus post-trial, $p = 0.8006$; during-trial versus post-trial, $p = 0.9493$. ***F,*** Proportion of time the toe remained above threshold during each trial phase (saline, 1.2 mA; $n = 4$). Each point represents the mean value for a single animal, averaged across multiple trials. Each line connects the mean values from the same subject. *Comparisons,* pre-trial versus during-trial, $p = 0.0830$; pre-trial versus post-trial, $p = 0.5411$; during-trial versus post-trial, $p = 0.1205$. *Statistical analysis,* repeated-measures one-way ANOVA with Tukey's multiple comparisons test. $*p < 0.05$; $**p < 0.01$; $***p < 0.001$; otherwise not statistically significant.

3.2 Closed-loop stimulation induces spinal motor learning

To assess whether closed-loop stimulation of the saphenous nerve can induce spinal motor learning, we trained mice to raise their left hindlimb at least 2 mm above its resting position. Figure 3 shows closed-loop and control trials after saline administration with 1.2 mA stimulations. In the learner mouse (Figs. 3A-C), the toe position rapidly increased above threshold with stimulation and was maintained throughout the trial and post-trial period with only intermittent stimulation required. The control mouse (Figs. 3D-F) did not sustain toe elevation above threshold. Across animals (n = 8), learner mice exhibited significantly higher toe positions during the trial (p = 0.0004, one-way ANOVA) and post-trial (p = 0.0427) compared to pre-trial baseline (Fig. 3B). Also, the proportion of time the toe was maintained above threshold was significantly increased during the trial (Fig. 3C; n = 4; p = 0.0061; one-way ANOVA) and after the trial (p = 0.0419) compared to pre-trial.

In the control group, no significant differences were observed in the average toe positions (Fig. 2E; n = 8; all $p > 0.7057$; one-way ANOVA) or the time the toe remained above threshold (Fig. 2F; n = 4; all $p > 0.0830$; one-way ANOVA). These results demonstrate that closed-loop stimulation contingent on limb position induces robust spinal motor learning, as evidenced by sustained elevation of toe position. Control stimulation trials, even at a 1.2 mA current—4 times higher than the threshold and is expected to recruit Aβ, Aδ and C fibres—does not produce this effect, confirming that learning depends on the contingency of the stimulation.

Saline | Closed-loop stimulation | 0.3 mA

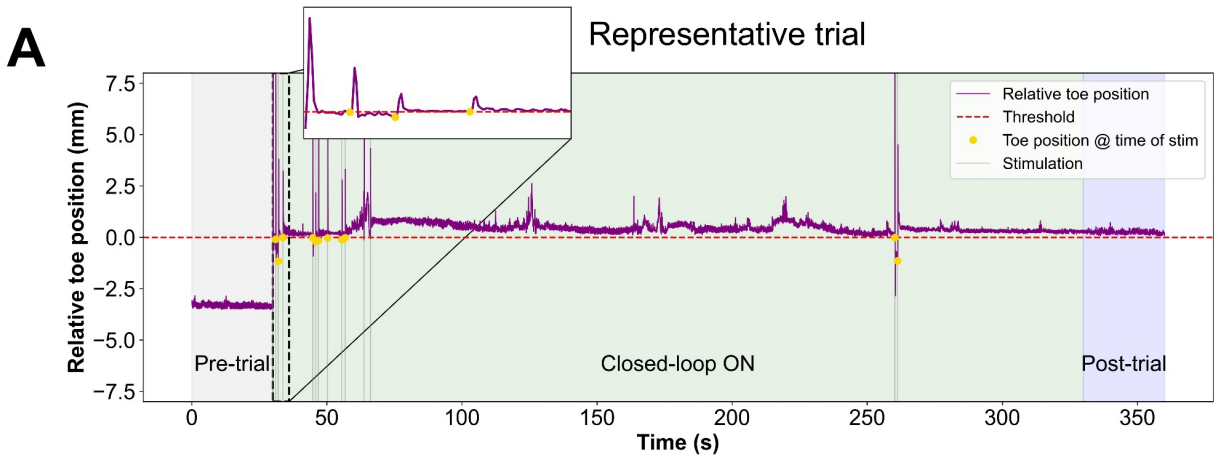

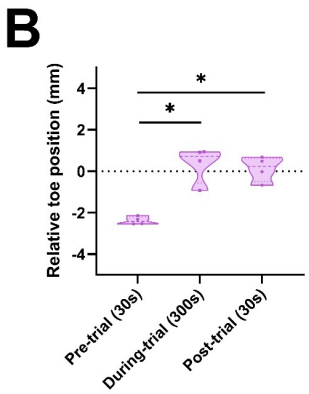

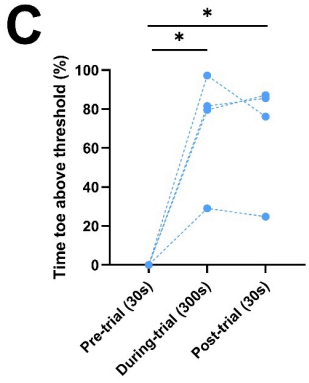

Saline | Closed-loop stimulation | 0.6 mA

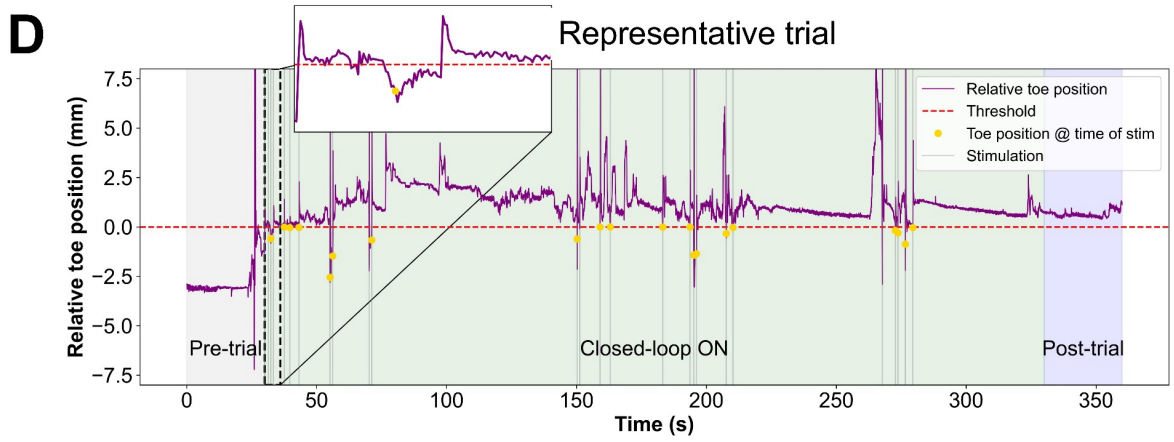

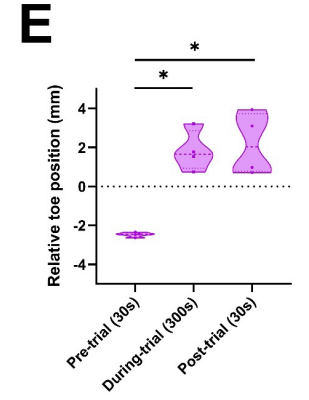

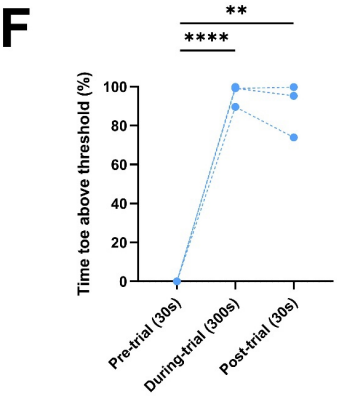

Figure 4: Closed-loop trials at 0.3 mA and 0.6 stimulations with saline administration. ***A,*** Representative trace of toe position during a closed-loop stimulation trial at 0.3 mA stimulations with saline administration. Stimulation times are indicated by vertical gray lines, with yellow dots marking toe position at the moment of stimulation. ***B, E,*** Average toe vertical position across trial phases in closed-loop stimulation trials at 0.3 mA (n = 4) and 0.6 mA (n = 4) stimulations with saline administration. Each point represents the mean value for a single animal, averaged across multiple trials. ***C, F,*** Proportion of time the toe remained above threshold during each trial phase with 0.3 mA (n = 4), 0.6 mA (n = 4) stimulations, respectively, with saline administration. Each line connects the mean values from the same subject. ***D,*** Representative trace of toe position during a closed-loop stimulation trial at 0.6 mA stimulations with saline administration. *Comparisons,* ***B,*** pre-trial versus during-trial, p = 0.0262; pre-trial versus post-trial, p = 0.0139; during-trial versus post-trial, p = 0.7037. ***E,*** pre-trial versus during-trial, p = 0.0081; pre-trial versus post-trial, p = 0.0229; during-trial versus post-trial, p = 0.6838. ***C,*** pre-trial versus during-trial, p = 0.0337; pre-trial versus post-trial, p = 0.0379; during-trial versus post-trial, p = 0.8595. ***F,*** pre-trial versus during-trial, $p < 0.0001$; pre-trial versus post-trial, p = 0.0014; during-trial versus post-trial, p = 0.5423. *Statistical analysis,* repeated-measures one-way ANOVA with Tukey's multiple comparisons test. *$p < 0.05$; **$p < 0.01$; ****$p < 0.0001$; otherwise not statistically significant.

3.3 Closed-loop stimulation induces motor learning across stimulation intensities

To assess whether closed-loop stimulation can induce motor learning at different stimulation intensities, we conducted trials at both 0.3 mA and 0.6 mA with saline administration. The 0.3 mA current was the threshold at which caused reflexive response in the hindlimb and is expected to correspond to the activation threshold for Aβ fibers (LTMRs), while 0.6 mA, which is 2 times the threshold, is expected to additionally recruit Aδ fibers (Koga et al., 2005). Since the control stimulation experiment with 1.2 mA already confirmed that learning does depend on the contingency of the stimulation, we did not repeat these experiments for lower intensity stimulations.

Representative traces (Figs. 4A, 4D) show that, at both currents, animals elevated their toe position above threshold during the closed-loop stimulation period, with this effect persisting into the post-trial phase. Quantitative analysis revealed that, at 0.3 mA, the average toe position was significantly higher during the trial (Fig. 4B; $n = 4$; $p = 0.0262$; one-way ANOVA) and post-trial ($p = 0.0139$) compared to pre-trial baseline. Similarly, the proportion of time the toe remained above threshold increased significantly during (Fig. 4C; $n = 4$; $p = 0.0337$; one-way ANOVA) and after the trial ($p = 0.0379$) compared to pre-trial. At 0.6 mA, the average toe position was also significantly elevated during (Fig. 4E; $n = 4$; $p = 0.0081$; one-way ANOVA) and after the trial ($p = 0.0229$) relative to pre-trial, and the proportion of time above threshold was increased during (Fig. 4F; $n = 4$; $p < 0.0001$; one-way ANOVA) and after the trial ($p = 0.0014$) compared to pre-trial.

These results demonstrate that closed-loop stimulation reliably induces spinal motor learning at both 0.3 mA and 0.6 mA stimulation intensities, suggesting that recruitment of only Aβ or Aβ with Aδ fibres can also induce motor learning.

J60 | Closed-loop stimulation | 1.2 mA

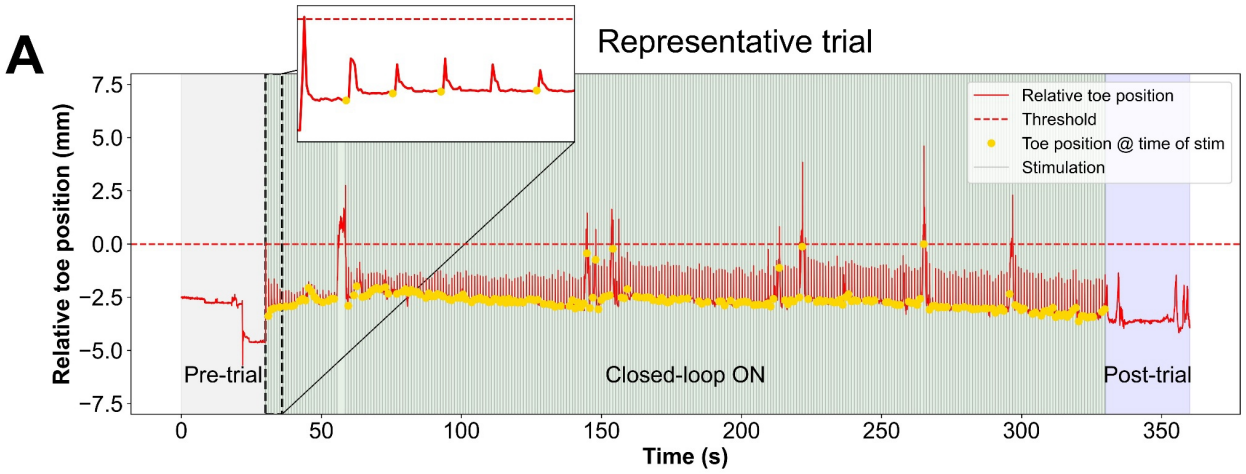

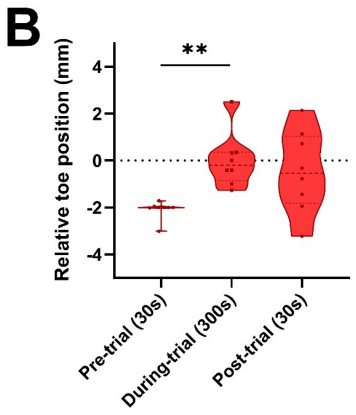

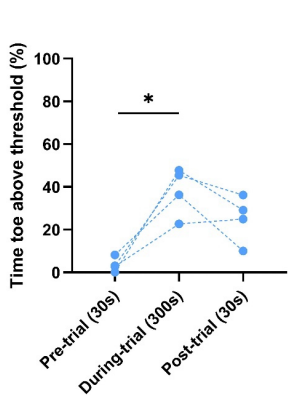

J60 | Control stimulation | 1.2 mA

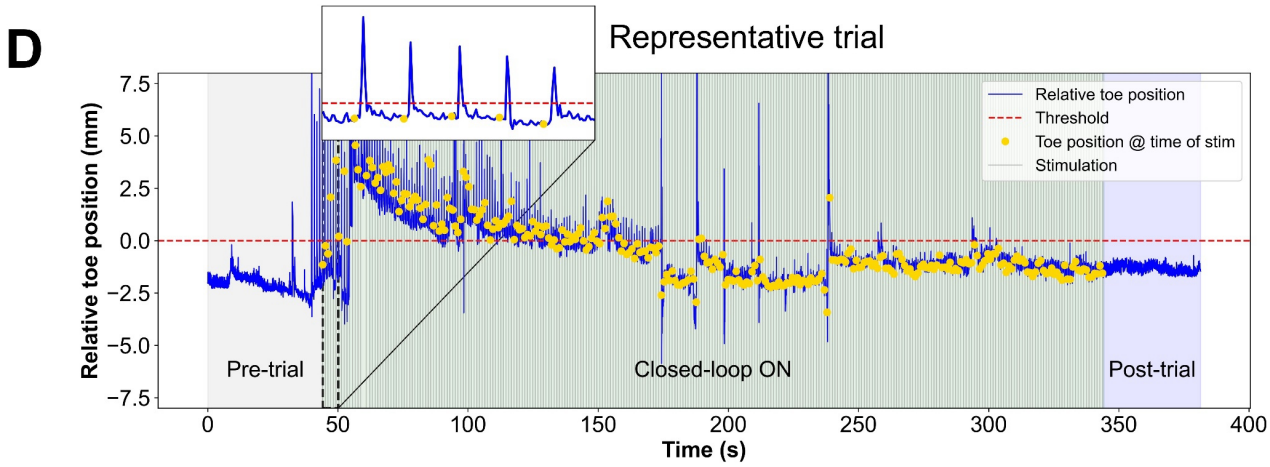

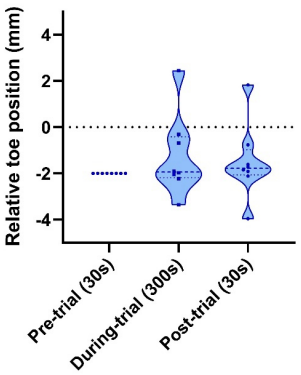

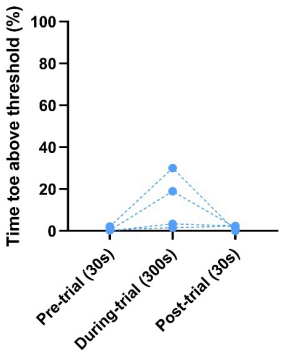

Figure 5: Closed-loop and control trials at 1.2 mA stimulations with J60 administration. ***A,*** Representative trace of toe position during a closed-loop stimulation trial (J60 administration with 1.2 mA stimulations). Stimulation times are indicated by vertical gray lines, with yellow dots marking toe position at the moment of stimulation. ***B,*** Average toe vertical position across trial phases in closed-loop stimulation trials (J60, 1.2 mA). Each point represents the mean value for a single animal, averaged across multiple trials ($n = 8$). *Comparisons,* pre-trial versus during-trial, $p = 0.0047$; pre-trial versus post-trial, $p = 0.0864$; during-trial versus post-trial, $p = 0.7880$. ***C,*** Proportion of time the toe remained above threshold during each trial phase with J60 and 1.2 mA stimulations. Each point represents the mean value for a single animal, averaged across multiple trials ($n = 4$). Each line connects the mean values from the same subject. *Comparisons,* pre-trial versus during-trial, $p = 0.0252$; pre-trial versus post-trial, $p = 0.1036$; during-trial versus post-trial, $p = 0.2353$. ***D,*** Control stimulation trial paired with the trial shown in panel A. The same stimulation times were delivered to this subject, but independently of toe position, administered with J60. ***E,*** Average toe vertical position across trial phases in control stimulation trials (J60, 1.2 mA; $n = 8$). *Comparisons,* pre-trial versus during-trial, $p = 0.4955$; pre-trial versus post-trial, $p = 0.6835$; during-trial versus post-trial, $p = 0.3303$. ***F,*** Proportion of time the toe remained above threshold during each trial phase (J60, 1.2 mA; $n = 4$). Each point represents the mean value for a single animal, averaged across multiple trials. Each line connects the mean values from the same subject. *Comparisons,* pre-trial versus during-trial, $p = 0.2610$; pre-trial versus post-trial, $p = 0.7104$; during-trial versus post-trial, $p = 0.3615$. *Statistical analysis,* repeated-measures one-way ANOVA with Tukey's multiple comparisons test. $*p < 0.05$; $**p < 0.01$; otherwise not statistically significant.

3.4 Silencing of hM4Di-expressing cells limits the expression of motor learning at 1.2 mA stimulation

To assess whether chemogenetic inhibition of hM4Di-expressing cells interferes with spinal motor learning at high stimulation intensity, we conducted closed-loop and control trials at 1.2 mA following J60 administration. In closed-loop trials (Fig. 5A), animals exhibited a significant elevation in average toe position during the stimulation period compared to the pre-trial baseline (Fig. 5B; $n = 8$; $p = 0.0047$, one-way ANOVA), suggesting that some degree of learning or adaptive response occurred. However, this improvement did not persist after stimulation ceased, as post-trial toe position was not significantly different from baseline ($p = 0.0864$). A similar pattern was observed for the proportion of time the toe remained above threshold (Fig. 5C; $n = 4$; $p = 0.0252$ during-trial vs. pre-trial; $p = 0.1036$ post-trial vs. pre-trial).

In control stimulation trials, there were no significant differences in toe position across any trial phase (Fig. 5E; all $p > 0.3303$). The proportion of time above threshold also did not differ significantly between phases (Fig. 5F; all $p > 0.2610$).

These findings suggest that although toe position improved during the stimulation period, the effects were short-lived and did not consolidate into longer-lasting post-trial changes. This pattern may reflect a transient or less stable form of motor learning that emerges during stimulation but fails to persist once stimulation ends. Another possibility is the acute, reflexive response to strong stimulation rather than true motor learning causes the toe to be above the threshold during the trial. Nonetheless, chemogenetic silencing of hM4Di-expressing cells prevents the toe to be elevated above the threshold in the post-trail period.

J60 | Closed-loop stimulation | 0.3 mA

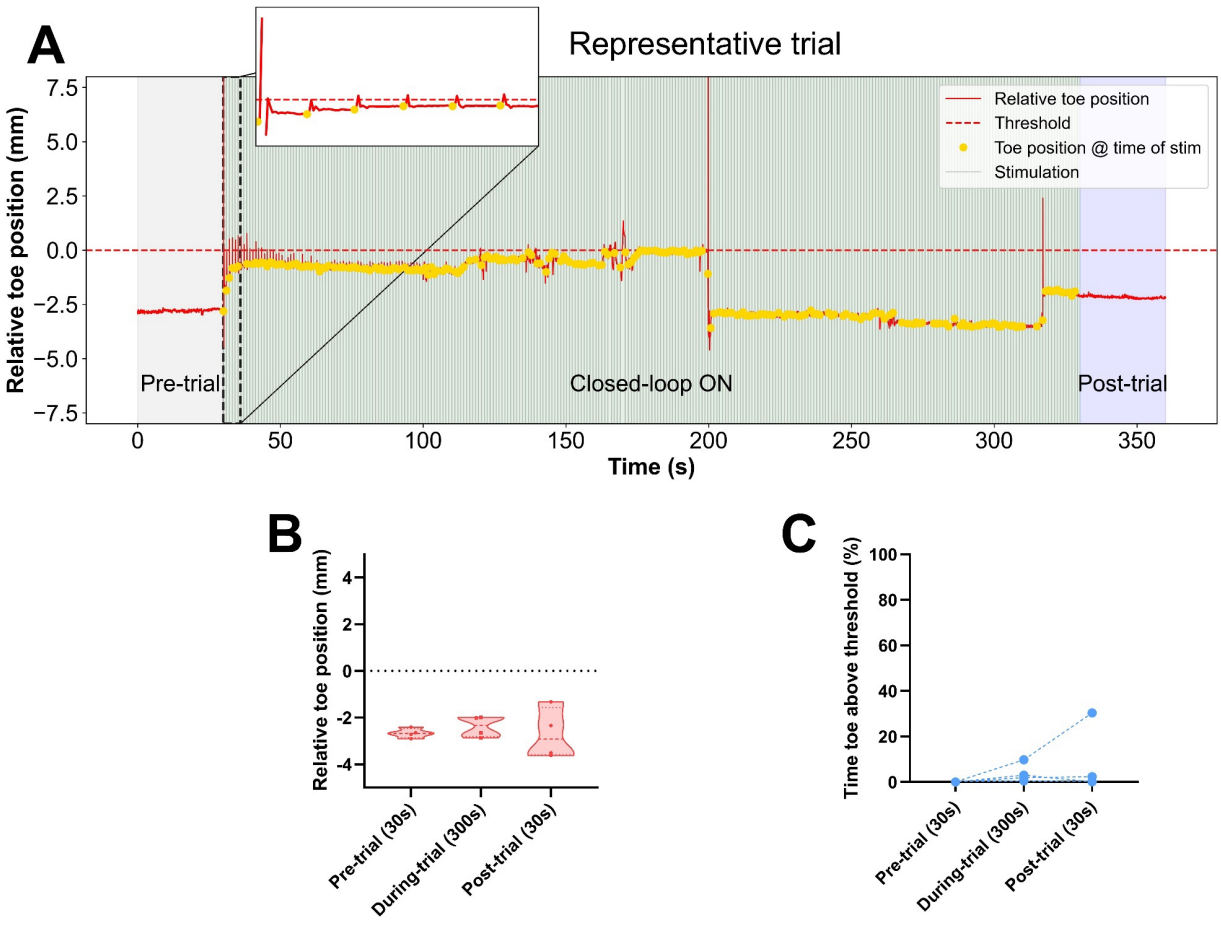

J60 | Closed-loop stimulation | 0.6 mA

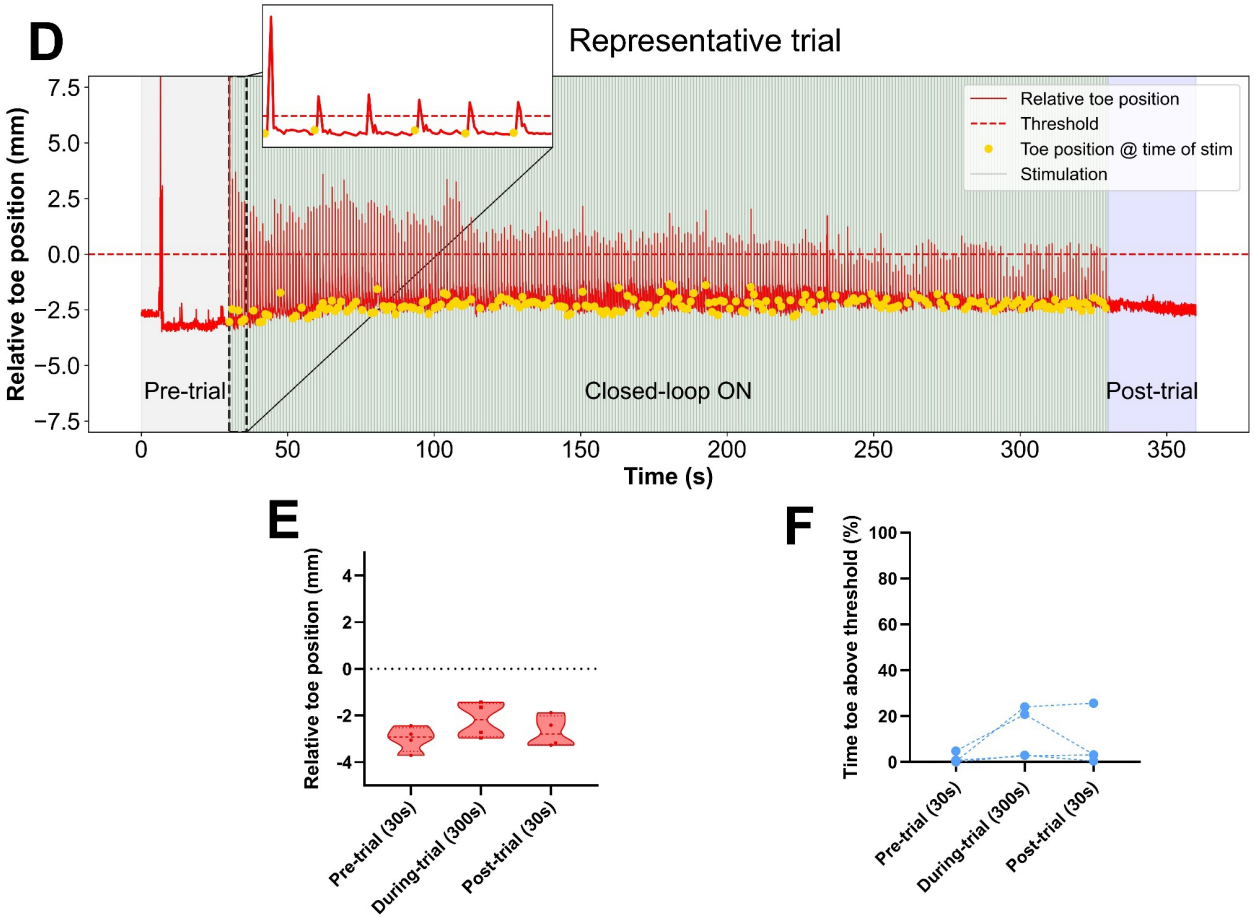

Figure 6: Closed-loop trials at 0.3 mA and 0.6 stimulations with J60 administration. ***A,*** Representative trace of toe position during a closed-loop stimulation trial at 0.3 mA stimulations with J60 administration. Stimulation times are indicated by vertical gray lines, with yellow dots marking toe position at the moment of stimulation. ***B, E,*** Average toe vertical position across trial phases in closed-loop stimulation trials at 0.3 mA ($n = 4$) and 0.6 mA ($n = 4$) stimulations with J60 administration. Each point represents the mean value for a single animal, averaged across multiple trials. ***C, F,*** Proportion of time the toe remained above threshold during each trial phase with 0.3 mA ($n = 4$), 0.6 mA ($n = 4$) stimulations, respectively, with J60 administration. Each line connects the mean values from the same subject. ***D,*** Representative trace of toe position during a closed-loop stimulation trial at 0.6 mA stimulations with J60 administration. *Comparisons,* ***B,*** pre-trial versus during-trial, $p = 0.6555$; pre-trial versus post-trial, $p = 0.9991$; during-trial versus post-trial, $p = 0.6856$. ***E,*** pre-trial versus during-trial, $p = 0.1243$; pre-trial versus post-trial, $p = 0.6870$; during-trial versus post-trial, $p = 0.1374$. ***C,*** pre-trial versus during-trial, $p = 0.3162$; pre-trial versus post-trial, $p = 0.5805$; during-trial versus post-trial, $p = 0.7238$. ***F,*** pre-trial versus during-trial, $p = 0.2365$; pre-trial versus post-trial, $p = 0.5967$; during-trial versus post-trial, $p = 0.6176$. *Statistical analysis,* repeated-measures one-way ANOVA with Tukey's multiple comparisons test. No statistically significant comparisons.

3.5 Silencing of hM4Di-expressing cells prevents motor learning at 0.6 mA and 0.3 mA stimulation

To determine whether chemogenetic inhibition of hM4Di-expressing neurons blocks the induction of spinal motor learning induced by stimulation of Abeta and Adelta afferents, we repeated the closed-loop stimulation paradigm at 0.3 mA and 0.6 mA following J60 administration. As in previous experiments, these currents were chosen to selectively recruit Aβ or Aβ with Aδ fibres, allowing us to assess the necessity of hM4Di-expressing neurons for learning across a range of sensory fiber activation.

Figure 6 presents representative closed-loop trials from three animals, each at a different stimulation current (0.3 and 0.6) in the presence of J60. In contrast to the saline condition, none of the animals maintained toe elevation above the threshold during or after the trial, regardless of stimulation intensity. The post-trial toe position remained below threshold in all cases, indicating a failure to acquire the motor learning task.

Quantitative analysis is shown in Figure 6. At both 0.3 mA and 0.6 mA, there was no significant increase in average toe position during or after the trial compared to pre-trial baseline (Figs. 6B, 6E, $n = 4$; all $p > 0.1243$, one-way ANOVA). Similarly, the proportion of time the toe was maintained above threshold did not differ significantly across trial phases at these currents (Figs. 6C, 6F; $n = 4$; $p > 0.2365$, one-way ANOVA).

Collectively, these results demonstrate that chemogenetic silencing of hM4Di-expressing neurons with J60 administration effectively prevents the acquisition of spinal motor learning at lower stimulation currents, where Aβ or Aβ with Aδ fibres are likely recruited.

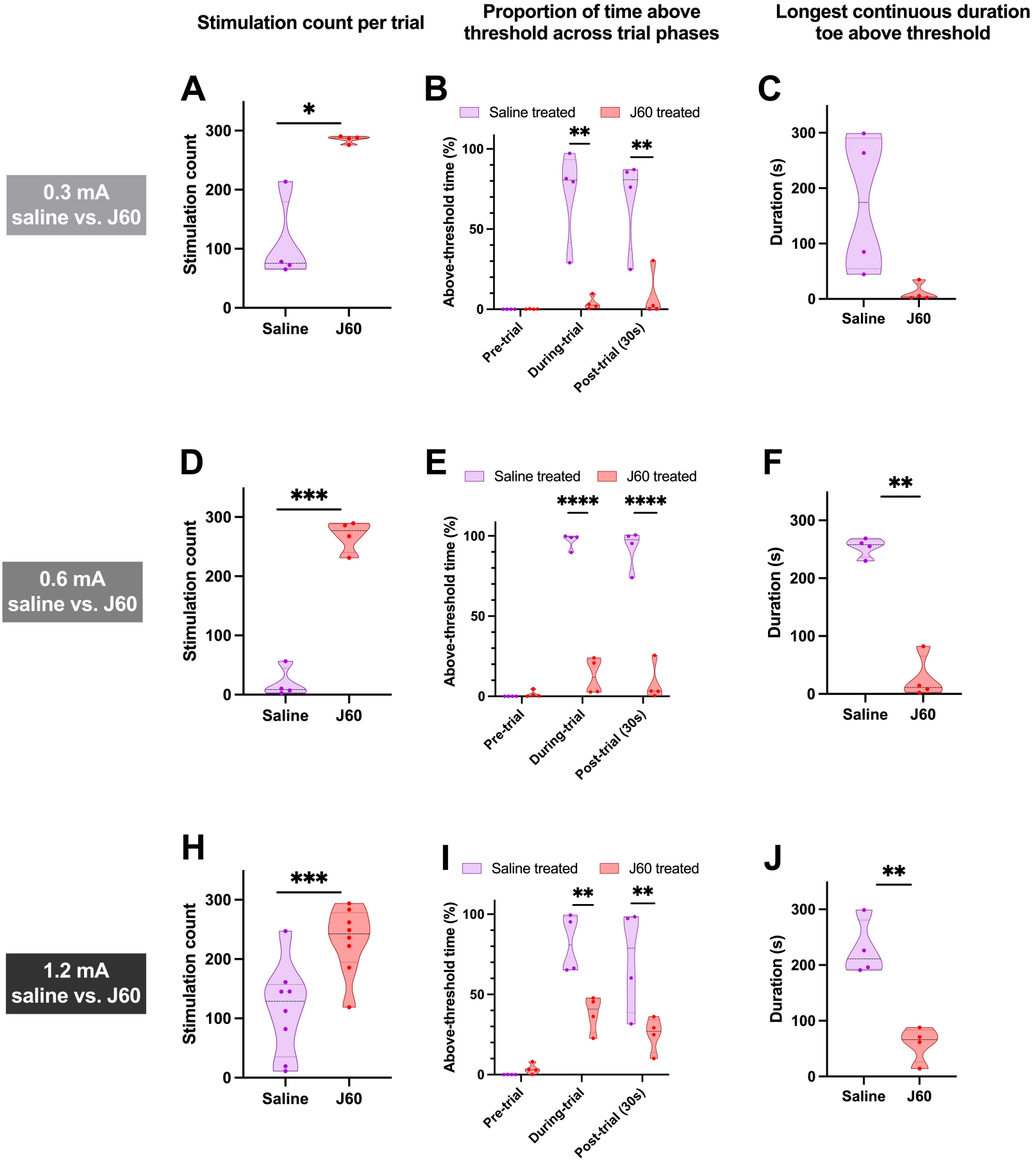
Stimulation count per trial
Proportion of time above threshold across trial phases
Longest continuous duration toe above threshold
0.3 mA saline vs. J60
0.6 mA saline vs. J60
1.2 mA saline vs. J60
A
B
C
D
E
F
H
I
J
Stimulation count
Above-threshold time (%)
Duration (s)
Saline
J60
Saline treated
J60 treated
Pre-trial
During-trial
Post-trial (30s)
*
**
***
****

Figure 7: Stimulation count and toe elevation metrics across stimulation currents and saline or J60 treatments. ***A, D, H,*** Stimulation count per trial at 0.3 mA (n = 4), 0.6 mA (n=4), and 1.2 mA (n = 8) stimulation currents, respectively, with either saline or J60 administration. Each point represents the mean number of stimulations an animal received in one trial (300s), averaged across multiple trials. The saline and J60 groups include the same animals. ***B, E, I,*** Proportion of time the toe remained above threshold during each trial phase with 0.3 mA (n = 4), 0.6 mA (n = 4) and 1.2 mA (n = 8) stimulation currents, respectively, with either saline or J60 administration. Each point represents the mean value for a single animal, averaged across multiple trials. The saline and J60 groups include the same animals. ***C, F, J,*** Longest continuous duration that the toe was held above threshold with 0.3 mA (n = 4), 0.6 mA (n = 4) and 1.2 mA (n = 8) stimulation currents, respectively, with either saline or J60 administration. Each point represents the maximum value that an animal held the toe above the threshold across any trial with the corresponding stimulation current and the drug given. The saline and J60 groups include the same animals. *Comparisons,* ***A,*** saline versus J60, $p = 0.0149$. ***D,*** saline versus J60, $p = 0.0004$. ***H,*** saline versus J60, $p = 0.0001$. ***B,*** saline versus J60 (pre-trial), $p > 0.9999$; saline versus J60 (during-trial), $p = 0.0012$; saline versus J60 (post-trial), $p = 0.0024$. ***E,*** saline versus J60 (pre-trial), $p = 0.9798$; saline versus J60 (during-trial), $p < 0.0001$; saline versus J60 (post-trial), $p < 0.0001$. ***I,*** saline versus J60 (pre-trial), $p = 0.9653$; saline versus J60 (during-trial), $p = 0.0048$; saline versus J60 (post-trial), $p = 0.0033$. ***C,*** saline versus J60, $p = 0.0982$. ***F,*** saline versus J60, $p = 0.0013$. ***J,*** saline versus J60, $p = 0.0044$. *Statistical analysis,* Repeated-measures two-way ANOVA with Sidak's multiple comparisons test. $^{**}p < 0.01$; $^{****}p < 0.0001$; otherwise not statistically significant (***B, E, I***). Two-tailed, paired t test. $^{*}p < 0.05$; $^{**}p < 0.01$; $^{****}p < 0.0001$; otherwise not statistically significant (***A, D, H, C, F, J***).

3.6 Comparison of Closed-Loop Stimulation Outcomes Between Saline and J60 Treatments

Next, we directly compared closed-loop stimulation performance between saline and J60 administration within the same cohort of mice, tested at different time points (Fig. 7). Trials were grouped by stimulation intensity: 0.3 mA (Figs. 7A–C; $n = 4$), 0.6 mA (Figs. 7D–F; $n = 4$), and 1.2 mA (Figs. 7H–J; $n = 8$).

To quantify motor learning, we assessed three key parameters: the total number of stimulations delivered during each 300-second trial (stimulation count), the proportion of time the toe was maintained above the threshold (above-threshold time), and the longest continuous duration the toe was held above threshold during any trial for each animal. A lower stimulation count suggests more effective learning since stimulations are only delivered when the toe is below the threshold. Also, because stimulation was delivered at 1 Hz, the maximum possible number of stimulations per trial was 300.

Across all stimulation intensities, saline-treated mice required significantly fewer stimulations than J60-treated mice (0.3 mA: Fig. 7A, $p = 0.0149$; 0.6 mA: Fig. 7D, $p = 0.0004$; 1.2 mA: Fig. 7H, $p = 0.0001$; t-tests). Similarly, the proportion of time the toe was maintained above threshold during the trial was significantly greater with saline than with J60 at all currents (0.3 mA: Fig. 7B, $p = 0.0012$; 0.6 mA: Fig. 7E, $p < 0.0001$; 1.2 mA: Fig. 7I, $p = 0.0048$; two-way ANOVA). This effect persisted into the post-trial period (0.3 mA: $p = 0.0024$; 0.6 mA: $p < 0.0001$; 1.2 mA: $p = 0.0033$). For the longest continuous duration, the toe was held above threshold, saline-treated mice outperformed J60-treated mice at 0.6 mA (Fig. 7F, $p = 0.0013$) and 1.2 mA (Fig. 7J, $p = 0.0044$), with a non-significant trend at 0.3 mA (Fig. 7C, $p = 0.0982$). Notably, the maximum

continuous durations observed with saline across all the animals were 298.74 s (0.3 mA), 268.77 s (0.6 mA), and 298.73 s (1.2 mA). This metric provides an additional measure of sustained motor performance, independent of the fixed 30-second post-trial window.

Collectively, these results demonstrate that J60 administration significantly increases stimulation requirements, reduces time above threshold, and shortens sustained toe elevation across all tested stimulation currents.

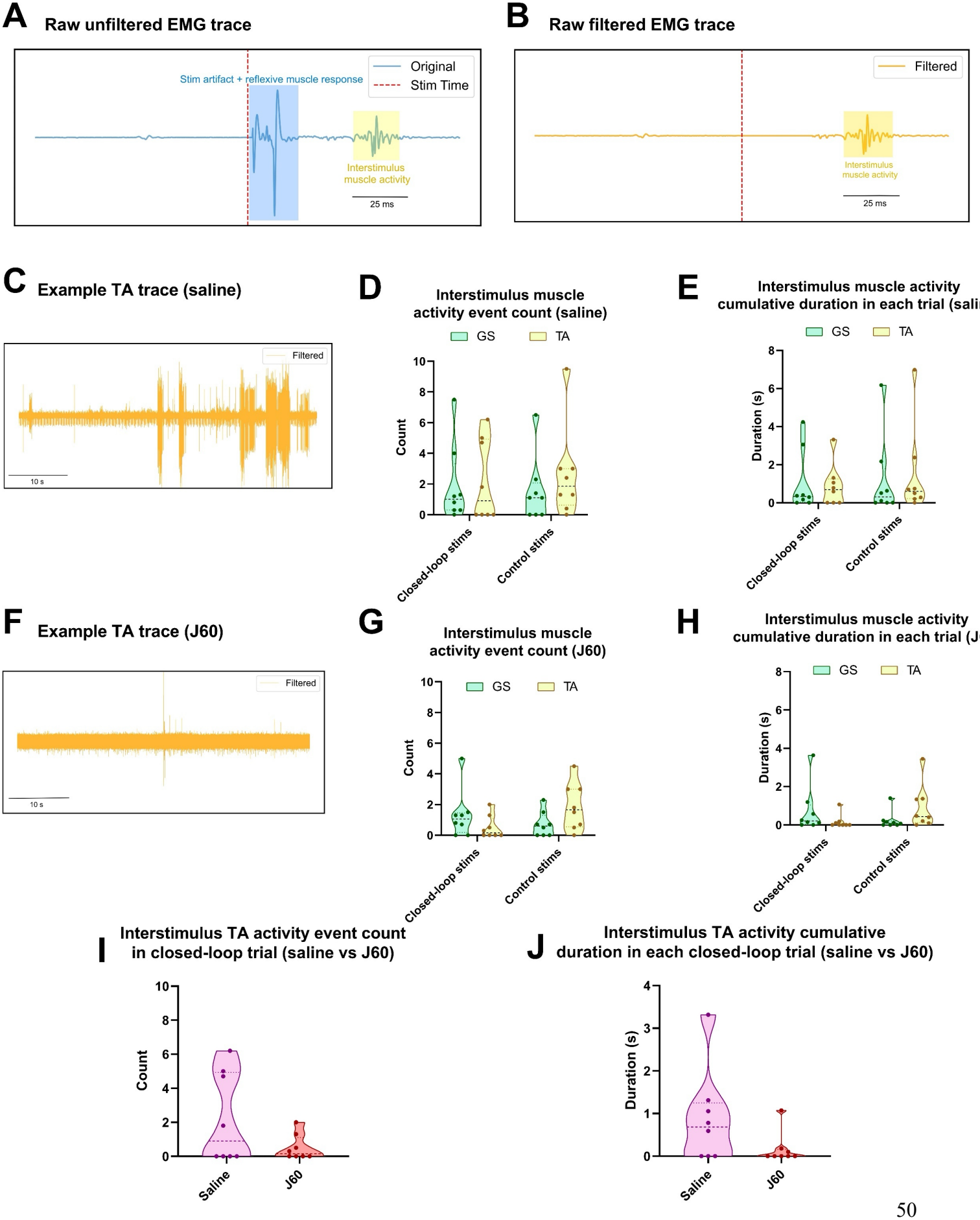
A
Raw unfiltered EMG trace
Stim artifact + reflexive muscle response
Original
Stim Time
Interstimulus muscle activity
25 ms
B
Raw filtered EMG trace
Filtered
Interstimulus muscle activity
25 ms
C
Example TA trace (saline)
Filtered
10 s
D
Interstimulus muscle activity event count (saline)
GS
TA
Count
Closed-loop stims
Control stims
E
Interstimulus muscle activity cumulative duration in each trial (saline)
GS
TA
Duration (s)
Closed-loop stims
Control stims
F
Example TA trace (J60)
Filtered
10 s
G
Interstimulus muscle activity event count (J60)
GS
TA
Count
Closed-loop stims
Control stims
H
Interstimulus muscle activity cumulative duration in each trial (J60)
GS
TA
Duration (s)
Closed-loop stims
Control stims
I
Interstimulus TA activity event count in closed-loop trial (saline vs J60)
Count
Saline
J60
J
Interstimulus TA activity cumulative duration in each closed-loop trial (saline vs J60)
Duration (s)
Saline
J60

Figure 8: Interstimulus muscle activity event count and cumulative duration of TA and GS in each trial with saline or J60 treatments. ***A, B,*** EMG trace with unfiltered and filtered stimulus artifact, respectively. The length of the stimulus itself was 9 ms and the signal was zeroed from the start of each stimulus event to 30 ms afterwards to filter the stimulus artifact and the short-latency muscle response to the stimulus. Each interstimulus muscle activity event was manually annotated. ***C, F,*** Representative filtered TA EMG trace with saline and J60 administration, respectively, both from the same animal. ***D, G, I,*** Interstimulus muscle activity event count of filtered EMG traces of TA and GS during closed-loop or control stimulation trials with either saline (n = 8) or J60 administration (n = 8). Each point represents the mean number of events within a single trial for an animal, averaged across multiple trials. The stimulation current for all of these trials was 1.2 mA. ***E, H, J,*** Interstimulus cumulative duration of muscle activity of filtered EMG traces of TA and GS within each closed-loop or control stimulation trial with either saline (n = 8) or J60 administration (n = 8). Each point represents the mean cumulative duration of events within a single trial for an animal, averaged across multiple trials. The stimulation current for all of these trials was 1.2 mA. *Comparisons,* ***D, E, G, H,*** no significance between any groups (6 comparisons). ***I,*** saline versus J60, p = 0.0647. ***J,*** saline versus J60, p = 0.1117. *Statistical analysis,* Repeated-measures two-way ANOVA with Sidak's multiple comparisons test. No comparison is statistically significant (***D, E, G, H, I, J***). Two-tailed, paired t test. No comparison is statistically significant (***I, J***).

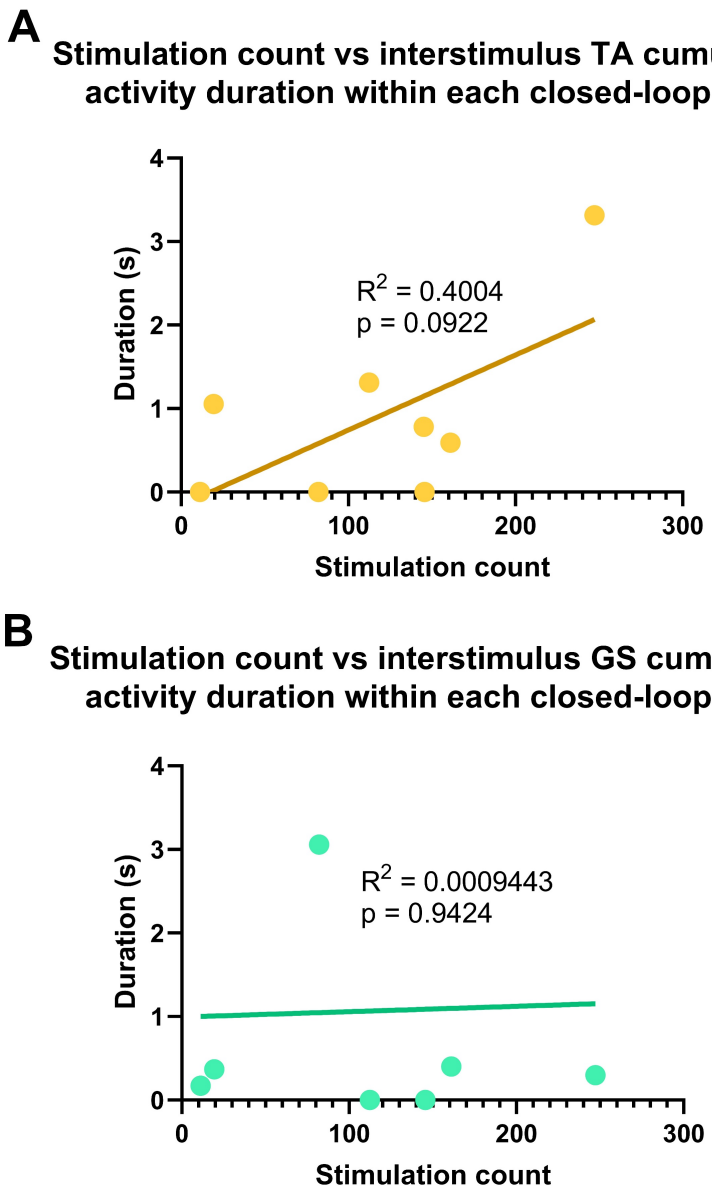

Figure 9: Stimulation count vs interstimulus muscle activity cumulative duration within each closed-loop trial. ***A, B,*** Stimulation count vs interstimulus TA and GS activity cumulative duration within each closed-loop. Each point represents the mean stimulation count of an animal averaged across multiple trials, and the mean TA activity cumulative duration (n = 8) and GS cumulative duration (n = 8) averaged across multiple trials. The stimulus current was 1.2 mA for all trials. *Statistical analysis,* ordinary least squares linear regresion of stimulation count versus cumulative duration. ***A,*** R^2 = 0.4004. Two-tailed t-test of whether the slope differs from zero: p = 0.0922. ***B,*** R^2 = 0.0009443. Two-tailed t-test of whether the slope differs from zero: p = 0.9424.

3.7 Assessing muscle activity during closed-loop trials

We next analyzed muscle activity during closed-loop and control stimulation trials (Fig. 8). Raw EMG traces from the TA and GS muscles exhibited prominent stimulus artifacts following saphenous nerve stimulation (Fig. 8A). To minimize contamination from these artifacts and short-latency reflex responses, the EMG signal was zeroed for 30 ms following each stimulus, effectively isolating muscle activity occurring between stimuli (Fig. 8B). This approach allowed for quantification of muscle activity related to long-latency responses, rather than short-latency responses. We focused our analysis on long-latency muscle activity (interstimulus muscle activity) because these events are not affected by stimulus artifacts.

Representative filtered TA EMG traces from saline- and J60-treated trials illustrate the typical patterns of interstimulus muscle activity observed in each condition (Figs. 8C, 8F). We analyzed the total number of interstimulus muscle activity events within one trial (Figs. 8D, 8G) and the cumulative interstimulus muscle activity duration within one trial (Figs. 8E, 8H). Quantitative analysis revealed no significant differences in interstimulus muscle activity event count or cumulative activity duration for either the TA or GS muscles between closed-loop and control stimulation trials under saline conditions, nor under J60 administration ($n = 8$; all $p > 0.05$, two-way ANOVA). Although visual inspection suggested a trend toward increased TA activity during saline treatment, statistical comparison of event count and cumulative duration in closed-loop trials showed no significant difference between saline and J60 groups (Figs. 8I, 8J; both $p > 0.0647$, t-tests).

To investigate whether TA or GS muscle activity contributed to successful toe elevation during the task, we examined the relationship between average stimulation count and average

cumulative muscle activity duration for each animal in closed-loop trials (Fig. 9). Linear regression analysis demonstrated no significant correlation between stimulation count and cumulative activity duration for either the TA (Fig. 9A; $R^2 = 0.4004$, $p = 0.0922$) or GS (Fig. 9B; $R^2 = 0.0009$, $p = 0.9424$) muscles. These findings suggest that the TA and GS muscles are not the primary contributors to toe elevation in this paradigm, which may explain the absence of significant differences in muscle activity across experimental conditions.

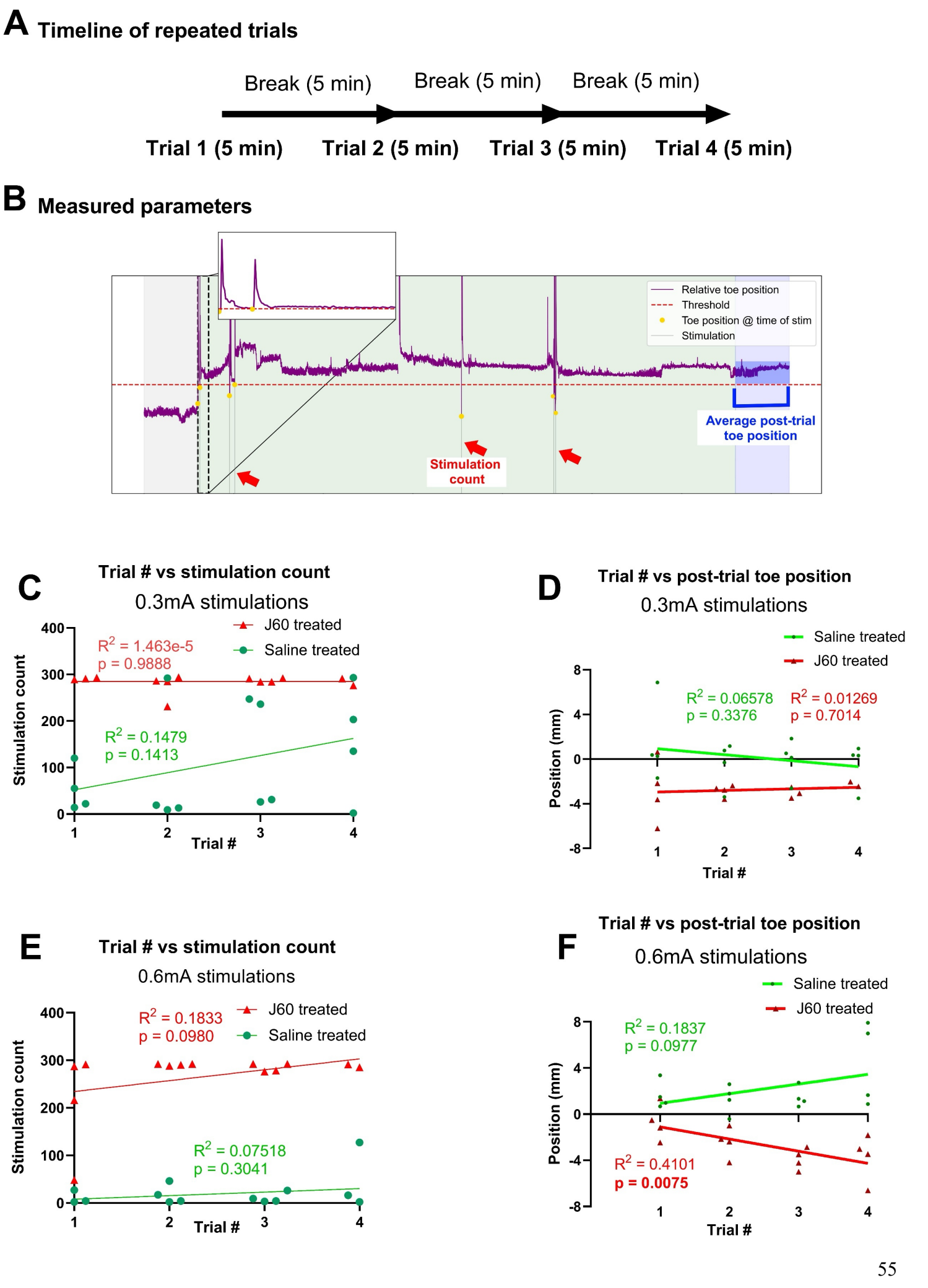
A Timeline of repeated trials
Break (5 min)
Break (5 min)
Break (5 min)
Trial 1 (5 min)
Trial 2 (5 min)
Trial 3 (5 min)
Trial 4 (5 min)
B Measured parameters
Relative toe position
Threshold
Toe position @ time of stim
Stimulation
Average post-trial toe position
Stimulation count
C
Trial # vs stimulation count
0.3mA stimulations
J60 treated
Saline treated
R2 = 1.463e-5
p = 0.9888
R2 = 0.1479
p = 0.1413
Stimulation count
Trial #
D
Trial # vs post-trial toe position
0.3mA stimulations
Saline treated
J60 treated
R2 = 0.06578
p = 0.3376
R2 = 0.01269
p = 0.7014
Position (mm)
Trial #
E
Trial # vs stimulation count
0.6mA stimulations
J60 treated
Saline treated
R2 = 0.1833
p = 0.0980
R2 = 0.07518
p = 0.3041
Stimulation count
Trial #
F
Trial # vs post-trial toe position
0.6mA stimulations
Saline treated
J60 treated
R2 = 0.1837
p = 0.0977
R2 = 0.4101
p = 0.0075
Position (mm)
Trial #

Figure 10: Effect of short-term repeated closed-loop trials on stimulation count and post-trial toe position at different stimulation currents with saline or J60 administration. ***A,*** Timeline of repeated closed-loop trials. Each animal underwent 4 closed-loop trials within 1 hour. ***B,*** Visualization of measured parameters: stimulation count and average post-trial toe position. ***C, E,*** Trial # vs stimulation count of the corresponding trial with 0.3 mA (n = 4) and 0.6 mA (n = 4) stimulation currents, respectively. Each point represents the stimulation count from the corresponding trial from a single animal. ***D, F,*** Trial # vs the average post-trial toe position of the corresponding trial with 0.3 mA (n = 4) and 0.6 mA (n = 4) stimulation currents, respectively. Each point represents the average toe position from the corresponding trial from a single animal. *Statistical analysis,* ordinary least squares linear regresion of trial # versus stimulation count or toe position. Two-tailed t-test of whether the slope differs from zero. R^2 values of linear regressions and p values of t-tests are reported on the figure.

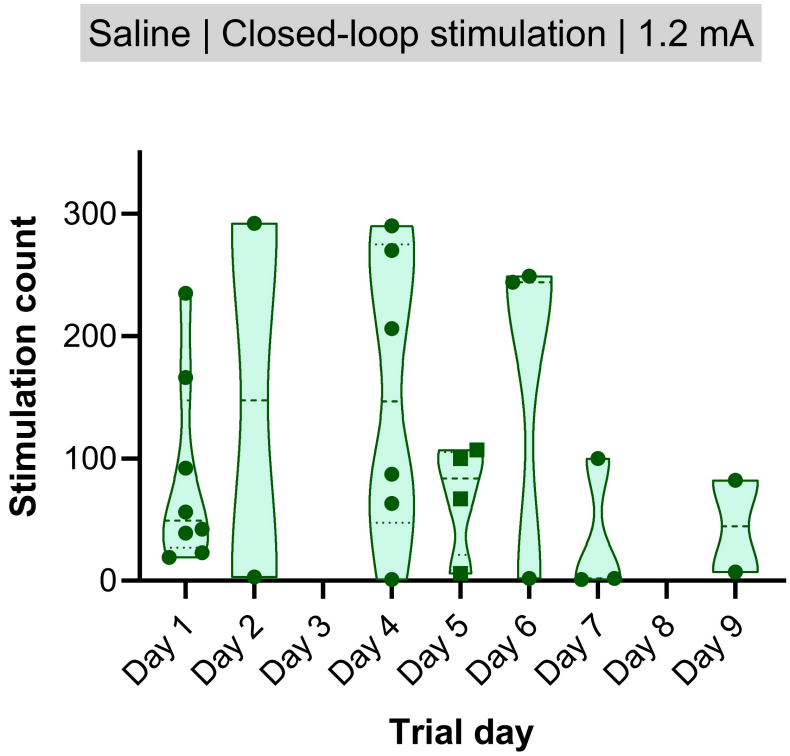

Figure 11: Effect of long-term repeated closed-loop trials on stimulation count. Each point represents the stimulation count from a single closed-loop trial of a single animal. Day 1 represents the first day the animal underwent the closed-loop trial. Subsequent trials were relative to Day 1. Day 1: $n = 8$; Day 2: $n = 2$; Day 3: $n = 0$; Day 4: $n = 6$; Day 5: $n = 4$; Day 6: $n = 3$; Day 7: $n = 3$; Day 8: $n = 0$; Day 9: $n = 2$. *Statistical analysis,* Mixed-effects model (REML) with trial day as a fixed effect and subject as a random effect. No significant effect of trial day on stimulation count was detected ($p > 0.05$). Matching (Chi-square test) was effective across animals ($p = 0.0108$)

3.8 Effect of repeated closed-loop trials on hindlimb behavior

To investigate the effects of repeated closed-loop stimulation on hindlimb behavior, we analyzed both short-term and long-term repetition using the same cohort of animals, with some missing values across days. For the short-term protocol (Fig. 10), mice underwent four consecutive closed-loop trials at either 0.3 mA or 0.6 mA, with 5-minute intervals between trials (Fig. 10A). We quantified two key parameters: the stimulation count per trial, which reflects how many stimulations were required for the mouse to learn to maintain the toe above threshold, and the post-trial toe position, which indicates whether the mouse retained the learned behavior after each trial (Fig. 10B). Linear regression analyses revealed no significant correlations between trial number and stimulation count or post-trial toe position at 0.3 mA for either saline- or J60-treated animals (Figs. 10C, 10D). Similarly, at 0.6 mA, there were no significant trends for stimulation count with saline administration (Figs. 10E). However, at 0.6 mA with J60 administration, a significant negative correlation was observed between trial number and post-trial toe position (Fig. 10F; $R^2 = 0.4101$, $p = 0.0075$), indicating a progressive decline in post-trial toe elevation across repeated trials. No other significant correlations were found, suggesting that, in most conditions, short-term repetition does not affect stimulation requirements or sustained limb position.

For the long-term protocol (Fig. 11), the same animals underwent daily closed-loop trials at 1.2 mA across up to nine days under saline conditions. Stimulation count was used as the primary outcome to assess changes in learning efficiency over time. Analysis revealed no significant differences in stimulation count across days ($p > 0.05$, mixed-effects model, REML), indicating

that the number of stimulations required to maintain the limb above threshold remained stable over the course of the experiment, despite some missing values on certain days.

Together, these results indicate that repeated closed-loop stimulation, whether within a single session or across multiple days, does not lead to systematic changes in the number of stimulations required or in the persistence of learned hindlimb elevation, except for a decline in post-trial toe position with repeated trials at 0.6 mA under J60 treatment.

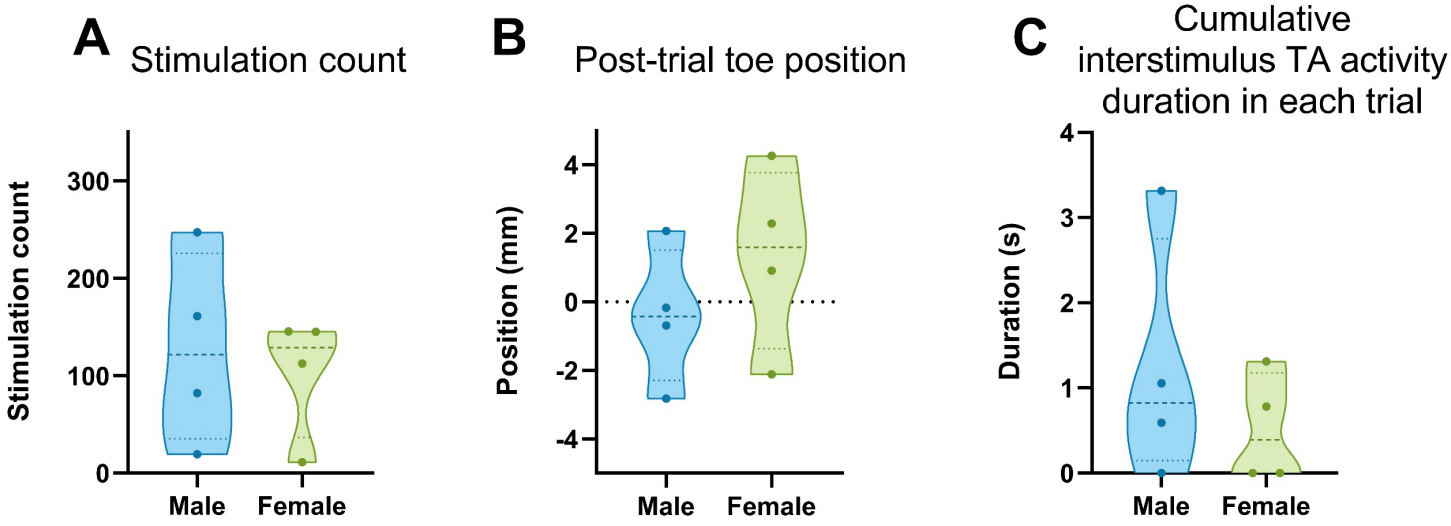

Figure 12: Effect of sex on stimulation count, post-trial toe position and cumulative interstimulus TA activity duration in each trial. ***A,*** Stimulation count of each trial for male (n = 4) and female (n = 4) mice. Each point represents the mean stimulation count for each animal, averaged across multiple trials with saline treatment and 1.2 mA stimulations. ***B,*** Post-trial toe position for male (n = 4) and female (n = 4) mice. Each point represents the mean post-trial toe position for each animal, averaged across multiple trials with saline treatment and 1.2 mA stimulations. ***C,*** Cumulative TA activity duration in each trial for male (n = 4) and female (n = 4) mice. Each point represents the mean duration for each animal, averaged across multiple trials with saline treatment and 1.2 mA stimulations. *Comparisons,* ***A,*** male versus female, p = 0.6980. ***B,*** male versus female, p = 0.3388. ***C,*** male versus female, p = 0.3998. *Statistical analysis,* Two-tailed, unpaired t test. No comparison is statistically significant (***A, B, C***).

3.9 Sex does not influence closed-loop motor learning metrics at 1.2 mA stimulation

Previous research has demonstrated that males and females can exhibit significant differences in pain perception and processing, with females often displaying greater pain sensitivity (Fillingim et al., 2009; Mogil, 2012). To assess whether sex influenced behavioral outcomes in our closed-loop learning paradigm, we focused our analysis on trials with 1.2 mA stimulations, a current intensity expected to robustly recruit both Aδ and C fibers, which transmit nociceptive signals (Kendroud et al., 2025). This group also provided the largest sample size (n = 8; 4 males and 4 females), while trials at lower currents (0.3 mA and 0.6 mA) included equal numbers of males and females but had a lower sample size (n = 4).

There were no significant differences between males and females in any of the primary outcome measures. Specifically, there were no differences in stimulation count per trial (Fig. 12A; n = 4 males, n = 4 females; p = 0.6980; unpaired t test), post-trial toe position (Fig. 12B; n = 4 males, n = 4 females; p = 0.3388; unpaired t test), or cumulative interstimulus TA activity duration within each trial (Fig. 12C; n = 4 males, n = 4 females; p = 0.3998; unpaired t test). These findings indicate that, despite well-established sex differences in pain processing, sex did not significantly affect the number of stimulations required, the persistence of learned hindlimb elevation, or cumulative muscle activity in our closed-loop paradigm under high-intensity stimulation conditions.

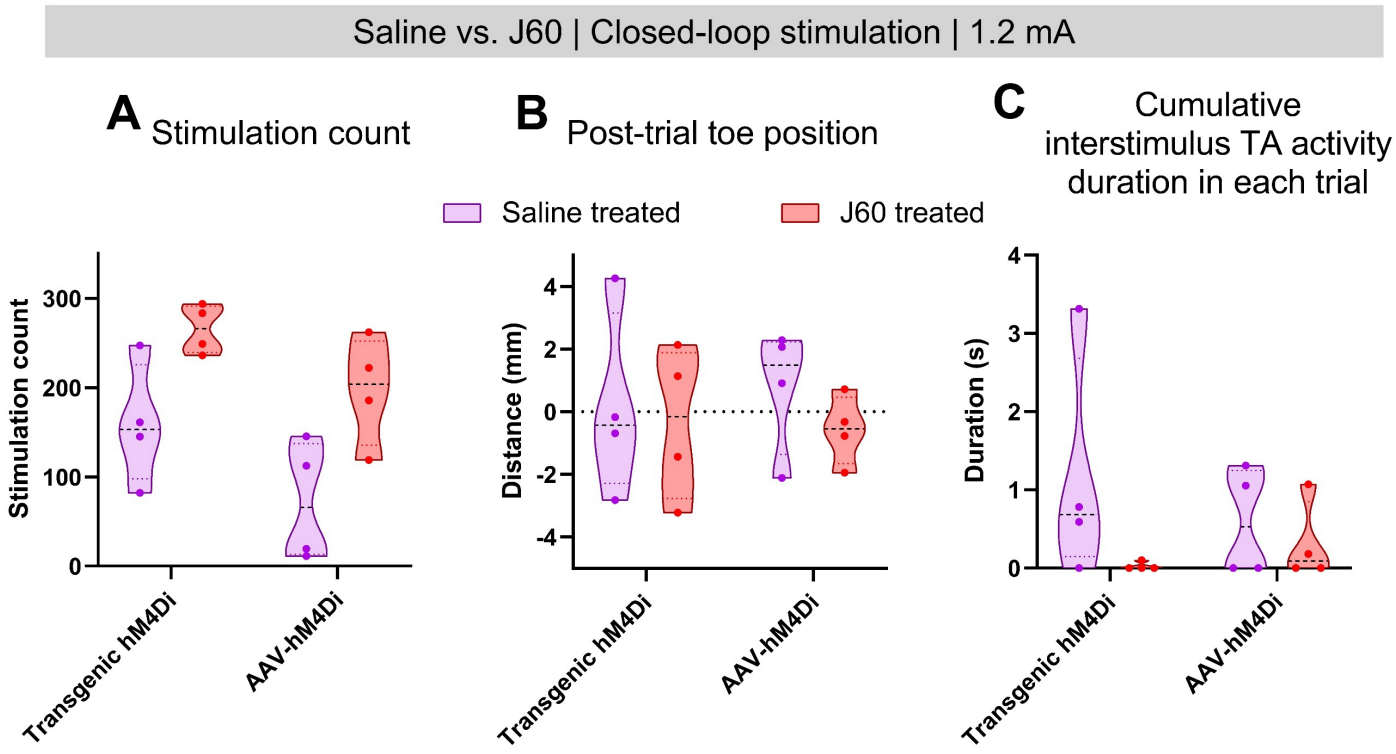

Figure 13: Effect of genetic differences on stimulation count, post-trial toe position and cumulative interstimulus TA activity duration in each trial. ***A,*** Stimulation count of each trial for transgenic hM4Di (n = 4) and AAV-hM4Di (n = 4) mice. Each point represents the mean stimulation count for each animal, averaged across multiple trials with saline treatment and 1.2 mA stimulations. ***B,*** Post-trial toe position for transgenic hM4Di (n = 4) and AAV-hM4Di (n = 4). Each point represents the mean post-trial toe position for each animal, averaged across multiple trials with saline treatment and 1.2 mA stimulations. ***C,*** Cumulative TA activity duration in each trial for transgenic hM4Di (n = 4) and AAV-hM4Di (n = 4) mice. Each point represents the mean duration for each animal, averaged across multiple trials with saline treatment and 1.2 mA stimulations. *Comparisons,* ***A,*** transgenic hM4Di versus AAV-hM4Di (saline treated), p = 0.1113; transgenic hM4Di versus AAV-hM4Di (J60 treated), p = 0.2299. ***B,*** transgenic hM4Di versus AAV-hM4Di (saline treated), p = 0.9050; transgenic hM4Di versus AAV-hM4Di (J60 treated), p = 0.9870. ***C,*** transgenic hM4Di versus AAV-hM4Di (saline treated), p = 0.5826; transgenic hM4Di versus AAV-hM4Di (J60 treated), p = 0.8711. *Statistical analysis,* Repeated-measures two-way ANOVA with Sidak's multiple comparisons test. No comparison is statistically significant (***A, B, C***).

3.10 Comparison of transgenic and AAV-mediated expression of hM4Di receptors in VGLUT2$^+$/Isl1$^+$ on motor learning metrics at 1.2 mA

To determine whether the method of expression of hM4Di receptors in VGLUT2$^+$/Isl1$^+$ cells (transgenic hM4Di and AAV-hM4Di) has an effect on our primary motor learning metrics, we compared the two groups during closed-loop trials at 1.2 mA with saline or J60 treatment (Fig. 13), which had the largest sample size (n = 8) compared to 0.6 mA (n = 4) or 0.3 mA (n = 4).

Across all primary outcome measures—stimulation count, post-trial toe position, and cumulative interstimulus TA activity duration—there were no significant differences between the two genetic groups. Specifically, stimulation count did not differ between transgenic and AAV-hM4Di mice with either saline (Fig. 13A; n = 4 males, n = 4 females; p = 0.1113; two-way ANOVA) or J60 treatment (p = 0.2299). Similarly, post-trial toe position was comparable between groups with saline (Fig. 13B; n = 4 males, n = 4 females; p = 0.9050; two-way ANOVA) or J60 treatment (p = 0.9870). Cumulative interstimulus TA activity duration also showed no significant group differences under saline (Fig. 13C; n = 4 males, n = 4 females; p = 0.5826; two-way ANOVA) or J60 treatment (p = 0.8711). These findings suggest that the method used to express hM4Di receptors in VGLUT2+/Isl1+ cells—whether transgenic or AAV-mediated—does not significantly impact motor learning metrics during closed-loop trials with 1.2 mA stimulations.

4.0 Discussion

4.1 dI3s are required for motor learning in the closed-loop paradigm

Our first objective was to determine whether dI3s are essential for motor learning in our closed-loop paradigm. To ensure the paradigm itself was effective, we first validated that closed-loop stimulation could indeed induce learning. In these experiments, each "learner" mouse was paired with a "control" mouse (Fig. 1). The key parameters for quantifying learning were the average toe position and the proportion of time the toe remained above threshold, measured during pre-trial, trial, and post-trial phases. We also quantified EMG parameters from the GS and TA muscles (Fig. 8); however, since we showed that their activity is not significantly correlated with toe elevation above the threshold (Fig. 9), we did not use EMG metrics to evaluate motor learning performance.

For learner mice, both the average toe position and the time above threshold were significantly higher during the trial and post-trial phases compared to pre-trial (Fig. 3B, 3C). In contrast, control mice did not show changes in these parameters across phases, indicating that learning depended on the contingency of the stimulation. This finding is consistent with prior work demonstrating that instrumental learning in the spinal cord requires a contingent relationship between behavior and stimulation (Buerger & Fennessy, 1971; Lavaud et al., 2024).

To directly test the requirement for dI3 neuron activity, we used DREADD (hM4Di) receptors, which have been shown to reliably hyperpolarize targeted neurons when activated by a designer drug (Roth, 2016). This approach allowed us to reversibly silence dI3 neurons within the same animal, enabling within-subject comparisons of motor learning with and without dI3 activity.

Unlike previous studies that relied on permanent ablation of related cell populations (Lavaud et al., 2024), our method provided temporal control over neuronal activity.

However, because both dI3s and a subset of nociceptive sensory afferents (Aδ and C fibres) express Isl1 and VGLUT2 (Goltash et al., 2025; Lagerström et al., 2010), our intersectional genetic strategy resulted in hM4Di expression in both populations (Fig. 2), which was a potential confound. Because we performed closed-loop trials at a stimulus intensity of 0.3 mA, which is at the behavioral threshold and selectively activates Aβ fibres, while Aδ and C fibres require approximately at least 2 and 4 times this threshold to be activated, respectively (Koga et al., 2005), off-target effects on nociceptors were minimized.

Comparisons therefore included closed-loop trials at 0.3 mA under both saline and J60 (DREADD agonist) conditions. With saline, learning was robust: both toe position and time above threshold increased during and after the trial (Fig. 4B, 4C). In contrast, J60 administration abolished these changes (Fig. 6B, 6C), and the number of stimulations required to elevate the toe (stimulation count) was significantly higher with J60 (Fig. 7A). Saline-treated mice maintained their toe above threshold significantly longer during and after the trial compared to J60-treated mice (Fig. 7B). Furthermore, repeated closed-loop trials at 0.3 mA with J60 did not reduce stimulation count or improve toe position across trials (Fig. 10C, 10D), confirming that motor learning was consistently prevented when dI3 activity was disrupted.

Collectively, these results strongly support the conclusion that dI3s are required for the acquisition of motor learning in this closed-loop toe elevation paradigm. The specificity of the effect at threshold stimulation, and the consistency across multiple behavioral metrics, underscore the critical role of dI3s in spinal motor plasticity.

4.2 Activation of low-threshold mechanoreceptors (LTMRs) alone is sufficient to drive spinal motor learning

Our second objective was to determine whether selective activation of LTMRs is sufficient to induce spinal motor learning. While previous studies have demonstrated the capacity for spinal motor learning (Buerger & Fennessy, 1971; Lavaud et al., 2024), the precise control of stimulation location and intensity was often lacking, making it difficult to attribute learning to specific sensory modalities. In this study, we addressed this limitation by stimulating the saphenous nerve—a cutaneous hindlimb nerve containing Aβ, Aδ, and C fibres (Abraira & Ginty, 2013; Milenkovic et al., 2008)—at defined current intensities to dissect the contributions of different afferent populations.

We selected three stimulation currents—0.3 mA, 0.6 mA, and 1.2 mA—to approximate the activation thresholds for Aβ, Aδ, and C fibres, respectively. At 0.3 mA, the threshold expected to selectively activate Aβ fibres, which are mostly LTMRs (Abraira & Ginty, 2013; Koga et al., 2005), both toe position and the proportion of time above threshold were significantly increased during and after the trial compared to pre-trial baseline (Figs. 4). This demonstrates that activation of LTMRs alone is sufficient to drive spinal motor learning. Since dI3s are known to receive direct input from LTMRs (Bui et al., 2013), we asked whether LTMRs could drive learning via alternative spinal circuits or whether dI3s are specifically required. At 0.3 mA, silencing of dI3s with J60 significantly increased the number of stimulations required to elevate the toe (stimulation count) and reduced the time the toe was maintained above threshold, compared to saline treatment (Figs. 7A, 7B). Although LTMRs are known to form synapses with a variety of excitatory and inhibitory interneurons (Abraira et al., 2017), our results indicate that the signals from LTMRs to dI3 pathway is essential for the induction of motor learning in this paradigm.

The question then becomes whether LTMRs are the sole contributors to learning, or whether Aδ/C fibres also play a role. Lavaud et al. (2024) examined the modulation of Aβ and Aδ/C fibres and found that learner mice, compared to those receiving control stimulations, showed a greater decrease in Aδ/C fibre response probability. This suggests that Aδ/C activity is suppressed as learning progresses. Therefore, even when we used higher stimulation intensities (0.6 or 1.2 mA) that likely recruited Aδ and C fibres, LTMRs may still have been the primary sensory modality supporting the learning process.

It is important to note, however, that due to off-target expression of hM4Di receptors in the superficial dorsal horn—likely corresponding to Aδ and C fibre terminals—J60 administration may also hyperpolarize and inhibit these nociceptive afferents. As a result, at 0.6 and 1.2 mA, which would normally activate Aδ/C fibres, these fibres were likely silenced. Since learning was not observed at these higher currents (Figs. 5, 6), this raises the question of whether this was due to inhibition of dI3s, Aδ/C fibres, or both. Given that Aδ/C fibre activity is already expected to decrease during learning—as shown by Lavaud et al. (2024)—it is more plausible that the lack of learning at higher currents reflects the absence of dI3 activity, rather than a critical role for Aδ/C fibres. Nonetheless, the off-target inhibition of Aδ/C fibres limits our ability to draw definitive conclusions about their role in motor learning.

4.3 Repetition of closed-loop trials with dI3 inhibition does not improve motor learning performance

Our final objective was to determine whether repeating closed-loop trials under dI3 inhibition could improve performance and induce motor learning over a longer timescale than the

standard 300-second trial. It is possible that dI3 inhibition does not abolish motor learning entirely, but simply delays its emergence. Even with saline administration, some animals required a greater number of stimulations over a longer period before maintaining their toe above threshold for extended durations (Fig. 4D), whereas others learned quickly, needing only a few stimulations at the start of the trial (Fig. 4A). Given this variability—and the fact that the 300-second trial duration is arbitrary, with no evidence that learning must occur within that timeframe—we repeated the closed-loop trials four times within a one-hour session (Fig. 10A). We evaluated performance based on stimulation count and post-trial toe position within each trial (Fig. 10B).

At 0.3 mA, J60-treated animals consistently received around 300 stimulations—the maximum possible during a 300-second trial due to the 1-second post-stimulation grace period—with no reduction across repeated trials (Fig. 10C). Similarly, post-trial toe positions remained below threshold across all four trials, with no sign of improvement (Fig. 10D). At 0.6 mA, there was a negative correlation between trial number and post-trial toe position in J60-treated mice (Fig. 10F). However, interpreting this trend is challenging due to potential off-target expression of hM4Di receptors in Aδ and C fibres and that 0.6 mA stimulations are expected to activate these fibres (Koga et al., 2005).

In summary, the absence of improvement in motor learning parameters across repeated 0.3 mA trials under dI3 inhibition further supports the idea that dI3s are required for the initial acquisition of spinal motor learning. Even with additional time and repeated exposure to the learning paradigm, motor learning could not be induced when dI3s were silenced.

4.4 Model of dI3s in motor learning

Building on our findings, we sought to explore how dI3s might contribute to motor learning at a conceptual level. Specifically, we propose that dI3s function as comparators—integrating feedforward and feedback signals to guide adaptive motor output. While this framework is well-established in studies of cerebellar motor learning, similar principles can be applied to the spinal cord. This section introduces the internal model framework and highlights its relevance to spinal circuits, drawing on prior work by Brownstone et al. (2015), who proposed a comparator-based model of spinal motor learning. We adopt a similar approach to interpret the role of dI3s in our paradigm.

Extensive research has shown that the cerebellum plays a central role in motor learning by predicting the sensory consequences of motor commands and adjusting behavior accordingly (Criscimagna-Hemminger et al., 2010; Gibo et al., 2013; Nguyen-Vu et al., 2013; Smith & Shadmehr, 2005; Synofzik et al., 2008; Taylor et al., 2010). For example, when learning to ride a bicycle, the cerebellum refines balance and steering by comparing predicted sensory outcomes—like the sensation of leaning—with actual sensory feedback, allowing the motor system to update commands and improve performance with practice.

This predictive control relies on internal models—neural representations used to estimate and evaluate the consequences of movement (Wolpert et al., 1998). Forward models use an efference copy of a motor command to predict its sensory outcome, enabling rapid, anticipatory adjustments before feedback arrives. For instance, when leaning left, the brain anticipates the bike's tilt and initiates corrective actions like shifting weight or steering, even before instability is sensed. Inverse models operate in the opposite direction, calculating the motor commands needed

to achieve a desired outcome—such as maintaining balance during a sudden tilt. Together, forward and inverse models allow for adaptive, feedforward control by enabling the brain to predict and correct for movement errors in real time (Wolpert et al., 1998).

Within the framework of internal models, we propose that dI3s function as comparators—integrating feedforward and feedback signals to drive motor learning. The concept of internal models in the spinal cord has been previously theorized. Brownstone et al. (2015) argued that spinal circuits are not limited to reflex execution but can support experience-dependent learning through internal evaluative mechanisms. Central to their model is a comparator circuit that receives both an efference copy of the motor command (feedforward signal) and actual sensory feedback. When there is a mismatch between predicted and actual feedback, a sensory prediction error is generated and used to update motor output, allowing the refinement of motor patterns over time. In our experiments, stimulation is delivered when muscle activity causes the toe to drop below a vertical threshold. The predicted sensory feedback—based solely on the animal's motor output—does not include this stimulation. When stimulation occurs, it introduces a mismatch between predicted and actual feedback. We hypothesize that dI3s detect this mismatch and drive adaptive changes in motor output to eliminate the error. As learning progresses and the hindlimb adjusts to keep the toe above threshold, stimulation stops, indicating that predicted and actual feedback have aligned and the error signal is resolved.

For dI3s to act as comparators, they must receive both sensory input from peripheral afferents and feedforward signals related to motor intent. Physiologically, this is plausible: dI3s receive input from proprioceptive, low-threshold cutaneous, and putatively nociceptive afferents (Bui et al., 2013), and project to motor neurons either directly or indirectly (Bui et al., 2016; Goltash et al., 2023; Nasiri et al., 2024). These properties position dI3s to detect mismatches

between expected and actual feedback and support their proposed role in spinal motor learning—consistent with both our findings and those of Lavaud et al. (2024).

Conclusion

This study demonstrates that dI3s are required for the acquisition of spinal motor learning in a closed-loop toe elevation paradigm. We show that silencing dI3s impairs learning even when low-threshold mechanoreceptors are selectively activated, and that performance does not improve with repeated trials under dI3 inhibition. These findings suggest that dI3s play a critical role in mediating the initial induction of learning. Building on this, we propose a conceptual model in which dI3s function as comparators—neurons that integrate feedforward and feedback signals to compute sensory prediction errors. This role would position dI3s as essential components of a spinal internal model architecture, supporting experience-dependent motor adaptation even in the absence of supraspinal input.

Bibliography

Abraira, V. E., & Ginty, D. D. (2013). The Sensory Neurons of Touch. *Neuron*, *79*(4), 10.1016/j.neuron.2013.07.051. https://doi.org/10.1016/j.neuron.2013.07.051

Abraira, V. E., Kuehn, E. D., Chirila, A. M., Springel, M. W., Toliver, A. A., Zimmerman, A. L., Orefice, L. L., Boyle, K. A., Bai, L., Song, B. J., Bashista, K. A., O'Neill, T. G., Zhuo, J., Tsan, C., Hoynoski, J., Rutlin, M., Kus, L., Niederkofler, V., Watanabe, M., … Ginty, D. D. (2017). The Cellular and Synaptic Architecture of the Mechanosensory Dorsal Horn. *Cell*, *168*(1–2), 295-310.e19. https://doi.org/10.1016/j.cell.2016.12.010

Adams, J. A. (1971). A Closed-Loop Theory of Motor Learning. *Journal of Motor Behavior*, *3*(2), Article 2. https://doi.org/10.1080/00222895.1971.10734898

Akay, T. (2014). Long-term measurement of muscle denervation and locomotor behavior in individual wild-type and ALS model mice. *Journal of Neurophysiology*, *111*(3), 694–703. https://doi.org/10.1152/jn.00507.2013

Akay, T., Acharya, H. J., Fouad, K., & Pearson, K. G. (2006). Behavioral and Electromyographic Characterization of Mice Lacking EphA4 Receptors. *Journal of Neurophysiology*, *96*(2), 642–651. https://doi.org/10.1152/jn.00174.2006

Alaynick, W. A., Jessell, T. M., & Pfaff, S. L. (2011). SnapShot: Spinal Cord Development. *Cell*, *146*(1), Article 1. https://doi.org/10.1016/j.cell.2011.06.038

Armstrong, S. A., & Herr, M. J. (2025). Physiology, Nociception. In *StatPearls*. StatPearls Publishing. http://www.ncbi.nlm.nih.gov/books/NBK551562/

Asan, A. S., McIntosh, J. R., & Carmel, J. B. (2022). Targeting Sensory and Motor Integration for Recovery of Movement After CNS Injury. *Frontiers in Neuroscience*, *15*, 791824. https://doi.org/10.3389/fnins.2021.791824

Bastian, A. J., Martin, T. A., Keating, J. G., & Thach, W. T. (1996). Cerebellar ataxia: Abnormal control of interaction torques across multiple joints. *Journal of Neurophysiology*, *76*(1), Article 1. https://doi.org/10.1152/jn.1996.76.1.492

Bear, M., Connors, B., & Paradiso, M. A. (2020). *Neuroscience: Exploring the Brain, Enhanced Edition: Exploring the Brain, Enhanced Edition*. Jones & Bartlett Learning.

Benevides, E. S., Thakre, P. P., Rana, S., Sunshine, M. D., Jensen, V. N., Oweiss, K., & Fuller, D. D. (2025). Chemogenetic stimulation of phrenic motor output and diaphragm activity. *eLife*, *13*, RP97846. https://doi.org/10.7554/eLife.97846

Brownstone, R. M., & Bui, T. V. (2010). Spinal interneurons providing input to the final common path during locomotion. *Progress in Brain Research*, *187*, 81–95. https://doi.org/10.1016/B978-0-444-53613-6.00006-X

Brownstone, R. M., Bui, T. V., & Stifani, N. (2015). Spinal circuits for motor learning. *Current Opinion in Neurobiology*, *33*, 166–173. https://doi.org/10.1016/j.conb.2015.04.007

Buerger, A. A., & Fennessy, A. (1971). Long-term alteration of leg position due to shock avoidance by spinal rats. *Experimental Neurology*, *30*(2), Article 2. https://doi.org/10.1016/S0014-4886(71)80001-8

Bui, T. V., Akay, T., Loubani, O., Hnasko, T. S., Jessell, T. M., & Brownstone, R. M. (2013a). Circuits for Grasping: Spinal dI3 Interneurons Mediate Cutaneous Control of Motor Behavior. *Neuron*, *78*(1), Article 1. https://doi.org/10.1016/j.neuron.2013.02.007

Bui, T. V., Akay, T., Loubani, O., Hnasko, T. S., Jessell, T. M., & Brownstone, R. M. (2013b). Circuits for grasping: Spinal dI3 interneurons mediate cutaneous control of motor behavior. *Neuron*, *78*(1), Article 1. https://doi.org/10.1016/j.neuron.2013.02.007

Bui, T. V., Stifani, N., Akay, T., & Brownstone, R. M. (2016). Spinal microcircuits comprising dI3 interneurons are necessary for motor functional recovery following spinal cord transection. *eLife*, *5*, e21715. https://doi.org/10.7554/eLife.21715

Bui, T. V., Stifani, N., Panek, I., & Farah, C. (2015). Genetically identified spinal interneurons integrating tactile afferents for motor control. *Journal of Neurophysiology*, *114*(6), Article 6. https://doi.org/10.1152/jn.00522.2015

Chad, D. A. (2003). Motor Control, Peripheral. In M. J. Aminoff & R. B. Daroff (Eds.), *Encyclopedia of the Neurological Sciences* (pp. 219–226). Academic Press. https://doi.org/10.1016/B0-12-226870-9/00813-3

Chapman, P. D., Kulkarni, A. S., Trevisan, A. J., Han, K., Hinton, J. M., Deltuvaite, P., Fenno, L. E., Ramakrishnan, C., Patton, M. H., Schwarz, L. A., Zakharenko, S. S., Deisseroth, K., & Bikoff, J. B. (2025). A brain-wide map of descending inputs onto spinal V1 interneurons. *Neuron*, *113*(4), 524-538.e6. https://doi.org/10.1016/j.neuron.2024.11.019

Cheng, L., Arata, A., Mizuguchi, R., Qian, Y., Karunaratne, A., Gray, P. A., Arata, S., Shirasawa, S., Bouchard, M., Luo, P., Chen, C.-L., Busslinger, M., Goulding, M., Onimaru, H., & Ma, Q. (2004). Tlx3 and Tlx1 are post-mitotic selector genes determining glutamatergic over GABAergic cell fates. *Nature Neuroscience*, *7*(5), Article 5. https://doi.org/10.1038/nn1221

Criscimagna-Hemminger, S. E., Bastian, A. J., & Shadmehr, R. (2010). Size of Error Affects Cerebellar Contributions to Motor Learning. *Journal of Neurophysiology*, *103*(4), Article 4. https://doi.org/10.1152/jn.00822.2009

de Leon, R. D., Hodgson, J. A., Roy, R. R., & Edgerton, V. R. (1998). Locomotor Capacity Attributable to Step Training Versus Spontaneous Recovery After Spinalization in Adult Cats. *Journal of Neurophysiology*, *79*(3), 1329–1340. https://doi.org/10.1152/jn.1998.79.3.1329

Dougherty, K. J., Zagoraiou, L., Satoh, D., Rozani, I., Doobar, S., Arber, S., Jessell, T. M., & Kiehn, O. (2013). Locomotor Rhythm Generation Linked to the Output of Spinal Shox2 Excitatory Interneurons. *Neuron*, *80*(4), 920–933. https://doi.org/10.1016/j.neuron.2013.08.015

Fillingim, R. B., King, C. D., Ribeiro-Dasilva, M. C., Rahim-Williams, B., & Riley, J. L. (2009). Sex, Gender, and Pain: A Review of Recent Clinical and Experimental Findings. *Journal of Pain*, *10*(5), 447–485. https://doi.org/10.1016/j.jpain.2008.12.001

Gibo, T. L., Criscimagna-Hemminger, S. E., Okamura, A. M., & Bastian, A. J. (2013). Cerebellar motor learning: Are environment dynamics more important than error size? *Journal of Neurophysiology*, *110*(2), Article 2. https://doi.org/10.1152/jn.00745.2012

Goltash, S., Khodr, R., Bui, T. V., & Laliberte, A. M. (2025). An optogenetic mouse model of hindlimb spasticity after spinal cord injury. *Experimental Neurology*, *386*, 115157. https://doi.org/10.1016/j.expneurol.2025.115157

Goltash, S., Stevens, S. J., Topcu, E., & Bui, T. V. (2023). Changes in synaptic inputs to dI3 INs and MNs after complete transection in adult mice. *Frontiers in Neural Circuits*, *17*. https://doi.org/10.3389/fncir.2023.1176310

Grau, J. W., Washburn, S. N., Hook, M. A., Ferguson, A. R., Crown, E. D., Garcia, G., Bolding, K. A., & Miranda, R. C. (2004). Uncontrollable stimulation undermines recovery after spinal cord injury. *Journal of Neurotrauma*, *21*(12), Article 12. https://doi.org/10.1089/neu.2004.21.1795

Grillner, S., & El Manira, A. (2020). Current Principles of Motor Control, with Special Reference to Vertebrate Locomotion. *Physiological Reviews*, *100*(1), 271–320. https://doi.org/10.1152/physrev.00015.2019

Guo, Z., Zhao, C., Huang, M., Huang, T., Fan, M., Xie, Z., Chen, Y., Zhao, X., Xia, G., Geng, J., & Cheng, L. (2012). Tlx1/3 and Ptf1a Control the Expression of Distinct Sets of Transmitter and Peptide Receptor Genes in the Developing Dorsal Spinal Cord. *Journal of Neuroscience*, *32*(25), Article 25. https://doi.org/10.1523/JNEUROSCI.6301-11.2012

Harding, E. K., Fung, S. W., & Bonin, R. P. (2020). Insights Into Spinal Dorsal Horn Circuit Function and Dysfunction Using Optical Approaches. *Frontiers in Neural Circuits*, *14*, 31. https://doi.org/10.3389/fncir.2020.00031

Kandel, E. R., Koester, J. D., Mack, S. H., & Siegelbaum, S. A. (2021). *Principles of Neural Science, Sixth Edition*. McGraw Hill Professional.

Kendroud, S., Fitzgerald, L. A., Murray, I. V., & Hanna, A. (2025). Physiology, Nociceptive Pathways. In *StatPearls*. StatPearls Publishing. http://www.ncbi.nlm.nih.gov/books/NBK470255/

Kent, J. A., Sommerfeld, J. H., Mukherjee, M., Takahashi, K. Z., & Stergiou, N. (2019). Locomotor patterns change over time during walking on an uneven surface. *The Journal of Experimental Biology*, *222*(14), Article 14. https://doi.org/10.1242/jeb.202093

Koga, K., Furue, H., Rashid, M. H., Takaki, A., Katafuchi, T., & Yoshimura, M. (2005). Selective activation of primary afferent fibers evaluated by sine-wave electrical stimulation. *Molecular Pain*, *1*, 13. https://doi.org/10.1186/1744-8069-1-13

Kondo, T., Sheets, P. L., Zopf, D. A., Aloor, H. L., Cummins, T. R., Chan, R. J., & Hashino, E. (2008). Tlx3 exerts context-dependent transcriptional regulation and promotes neuronal differentiation from

embryonic stem cells. *Proceedings of the National Academy of Sciences*, *105*(15), Article 15. https://doi.org/10.1073/pnas.0708704105

Krakauer, J. W., & Mazzoni, P. (2011). Human sensorimotor learning: Adaptation, skill, and beyond. *Current Opinion in Neurobiology*, *21*(4), Article 4. https://doi.org/10.1016/j.conb.2011.06.012

Kubasak, M. D., Jindrich, D. L., Zhong, H., Takeoka, A., McFarland, K. C., Muñoz-Quiles, C., Roy, R. R., Edgerton, V. R., Ramón-Cueto, A., & Phelps, P. E. (2008). OEG implantation and step training enhance hindlimb-stepping ability in adult spinal transected rats. *Brain*, *131*(1), 264–276. https://doi.org/10.1093/brain/awm267

Kwan, A. C., Dietz, S. B., Webb, W. W., & Harris-Warrick, R. M. (2009). Activity of Hb9 Interneurons during Fictive Locomotion in Mouse Spinal Cord. *Journal of Neuroscience*, *29*(37), 11601–11613. https://doi.org/10.1523/JNEUROSCI.1612-09.2009

Lagerström, M. C., Rogoz, K., Abrahamsen, B., Persson, E., Reinius, B., Nordenankar, K., Ölund, C., Smith, C., Mendez, J. A., Chen, Z.-F., Wood, J. N., Wallén-Mackenzie, Å., & Kullander, K. (2010). VGLUT2-Dependent Sensory Neurons in the TRPV1 Population Regulate Pain and Itch. *Neuron*, *68*(3), 529–542. https://doi.org/10.1016/j.neuron.2010.09.016

Lai, H. C., Seal, R. P., & Johnson, J. E. (2016). Making sense out of spinal cord somatosensory development. *Development (Cambridge, England)*, *143*(19), Article 19. https://doi.org/10.1242/dev.139592

Lavaud, S., Bichara, C., D'Andola, M., Yeh, S.-H., & Takeoka, A. (2024). Two inhibitory neuronal classes govern acquisition and recall of spinal sensorimotor adaptation. *Science*, *384*(6692), Article 6692. https://doi.org/10.1126/science.adf6801

Lavrov, I., Courtine, G., Dy, C. J., Brand, R. van den, Fong, A. J., Gerasimenko, Y., Zhong, H., Roy, R. R., & Edgerton, V. R. (2008). Facilitation of Stepping with Epidural Stimulation in Spinal Rats: Role of Sensory Input. *Journal of Neuroscience*, *28*(31), Article 31. https://doi.org/10.1523/JNEUROSCI.1069-08.2008

Lawson, K. A., Ruiz, C. M., & Mahler, S. V. (2023). A head-to-head comparison of two DREADD agonists for suppressing operant behavior in rats via VTA dopamine neuron inhibition. *Psychopharmacology*, *240*(10), 2101–2110. https://doi.org/10.1007/s00213-023-06429-0

Leblond, H., L'Espérance, M., Orsal, D., & Rossignol, S. (2003). Treadmill Locomotion in the Intact and Spinal Mouse. *Journal of Neuroscience*, *23*(36), Article 36. https://doi.org/10.1523/JNEUROSCI.23-36-11411.2003

Li, F., Eriksen, J., Finer-Moore, J., Chang, R., Nguyen, P., Bowen, A., Myasnikov, A., Yu, Z., Bulkley, D., Cheng, Y., Edwards, R. H., & Stroud, R. M. (2020). Ion transport and regulation in a synaptic vesicle glutamate transporter. *Science (New York, N.Y.)*, *368*(6493), Article 6493. https://doi.org/10.1126/science.aba9202

Liem, K. F., Tremml, G., & Jessell, T. M. (1997). A Role for the Roof Plate and Its Resident TGFβ-Related Proteins in Neuronal Patterning in the Dorsal Spinal Cord. *Cell*, *91*(1), 127–138. https://doi.org/10.1016/S0092-8674(01)80015-5

Light, A. R., & Perl, E. R. (1979). Spinal termination of functionally identified primary afferent neurons with slowly conducting myelinated fibers. *The Journal of Comparative Neurology*, *186*(2), 133–150. https://doi.org/10.1002/cne.901860203

Lovely, R. G., Gregor, R. J., Roy, R. R., & Edgerton, V. R. (1986). Effects of training on the recovery of full-weight-bearing stepping in the adult spinal cat. *Experimental Neurology*, *92*(2), 421–435. https://doi.org/10.1016/0014-4886(86)90094-4

Martinez, M., Delivet-Mongrain, H., Leblond, H., & Rossignol, S. (2012). Incomplete spinal cord injury promotes durable functional changes within the spinal locomotor circuitry. *Journal of Neurophysiology*, *108*(1), 124–134. https://doi.org/10.1152/jn.00073.2012

Mayer, W. P., & Akay, T. (2018). Stumbling corrective reaction elicited by mechanical and electrical stimulation of the saphenous nerve in walking mice. *Journal of Experimental Biology*, *221*(13), jeb178095. https://doi.org/10.1242/jeb.178095

Milenkovic, N., Wetzel, C., Moshourab, R., & Lewin, G. R. (2008). Speed and Temperature Dependences of Mechanotransduction in Afferent Fibers Recorded From the Mouse Saphenous Nerve. *Journal of Neurophysiology*, *100*(5), 2771–2783. https://doi.org/10.1152/jn.90799.2008

Mogil, J. S. (2012). Sex differences in pain and pain inhibition: Multiple explanations of a controversial phenomenon. *Nature Reviews Neuroscience*, *13*(12), 859–866. https://doi.org/10.1038/nrn3360

Mona, B., Villarreal, J., Savage, T. K., Kollipara, R. K., Boisvert, B. E., & Johnson, J. E. (2020). Positive autofeedback regulation of Ptf1a transcription generates the levels of PTF1A required to generate itch circuit neurons. *Genes & Development*, *34*(9–10), Article 9–10. https://doi.org/10.1101/gad.332577.119

Monteiro, F. A., Miranda, R. M., Samina, M. C., Dias, A. F., Raposo, A. A. S. F., Oliveira, P., Reguenga, C., Castro, D. S., & Lima, D. (2021). Tlx3 Exerts Direct Control in Specifying Excitatory Over Inhibitory Neurons in the Dorsal Spinal Cord. *Frontiers in Cell and Developmental Biology*, *9*, 642697. https://doi.org/10.3389/fcell.2021.642697

Morton, S. M., & Bastian, A. J. (2006). Cerebellar contributions to locomotor adaptations during splitbelt treadmill walking. *Journal of Neuroscience*, *26*(36), Article 36. Scopus. https://doi.org/10.1523/JNEUROSCI.2622-06.2006

Nasiri, S., Laliberte, A. M., & Bui, T. V. (2024). *Mapping of dI3 neuron sensorimotor circuits across the cervical and lumbar spinal cord* (p. 2024.11.17.624039). bioRxiv. https://doi.org/10.1101/2024.11.17.624039

Nguyen-Vu, T. D. B., Kimpo, R. R., Rinaldi, J. M., Kohli, A., Zeng, H., Deisseroth, K., & Raymond, J. L. (2013). Cerebellar Purkinje cell activity drives motor learning. *Nature Neuroscience*, *16*(12), Article 12. https://doi.org/10.1038/nn.3576

Nishida, K., Hoshino, M., Kawaguchi, Y., & Murakami, F. (2010). Ptf1a Directly Controls Expression of Immunoglobulin Superfamily Molecules Nephrin and Neph3 in the Developing Central Nervous System*. *Journal of Biological Chemistry*, *285*(1), Article 1. https://doi.org/10.1074/jbc.M109.060657

Obeidat, M. S., Samara, M. N., Nazzal, M. S., & Alali, A. E. (2023). The effects of different carrying methods on human gait parameters. *International Journal of Industrial Ergonomics*, *93*, 103403. https://doi.org/10.1016/j.ergon.2022.103403

Orsal, D., Barthe, J.-Y., Antri, M., Feraboli-Lohnherr, D., Yakovleff, A., y Ribotta, M. G., Privat, A., Provencher, J., & Rossignol, S. (2002). Chapter 16 Locomotor recovery in chronic spinal rat: Long-term pharmacological treatment or transplantation of embryonic neurons? In L. McKerracher, G. Doucet, & S. Rossignol (Eds.), *Progress in Brain Research* (Vol. 137, pp. 213–230). Elsevier. https://doi.org/10.1016/S0079-6123(02)37018-3

Osseward, P. J., & Pfaff, S. L. (2019). Cell type and circuit modules in the spinal cord. *Current Opinion in Neurobiology*, *56*, 175–184. https://doi.org/10.1016/j.conb.2019.03.003

Pan, Y.-Z., & Pan, H.-L. (2004). Primary Afferent Stimulation Differentially Potentiates Excitatory and Inhibitory Inputs to Spinal Lamina II Outer and Inner Neurons. *Journal of Neurophysiology*, *91*(6), 2413–2421. https://doi.org/10.1152/jn.01242.2003

Papathanou, M., Creed, M., Dorst, M. C., Bimpisidis, Z., Dumas, S., Pettersson, H., Bellone, C., Silberberg, G., Lüscher, C., & Wallén-Mackenzie, Å. (2018). Targeting VGLUT2 in Mature Dopamine Neurons Decreases Mesoaccumbal Glutamatergic Transmission and Identifies a Role for Glutamate Co-release in Synaptic Plasticity by Increasing Baseline AMPA/NMDA Ratio. *Frontiers in Neural Circuits*, *12*. https://doi.org/10.3389/fncir.2018.00064

Pearson, K. G., Acharya, H., & Fouad, K. (2005). A new electrode configuration for recording electromyographic activity in behaving mice. *Journal of Neuroscience Methods*, *148*(1), 36–42. https://doi.org/10.1016/j.jneumeth.2005.04.006

Racinais, S., & Oksa, J. (2010). Temperature and neuromuscular function. *Scandinavian Journal of Medicine & Science in Sports*, *20*(s3), Article s3. https://doi.org/10.1111/j.1600-0838.2010.01204.x

Rexed, B. (1952). The cytoarchitectonic organization of the spinal cord in the cat. *The Journal of Comparative Neurology*, *96*(3), Article 3. https://doi.org/10.1002/cne.900960303

Rivera-Arconada, I., Baccei, M. L., López-García, J. A., & Bardoni, R. (2025). An electrophysiologist's guide to dorsal horn excitability and pain. *Frontiers in Cellular Neuroscience*, *19*, 1548252. https://doi.org/10.3389/fncel.2025.1548252

Rossignol, S., & Frigon, A. (2011). Recovery of Locomotion After Spinal Cord Injury: Some Facts and Mechanisms. *Annual Review of Neuroscience*, *34*(Volume 34, 2011), Article Volume 34, 2011. https://doi.org/10.1146/annurev-neuro-061010-113746

Roth, B. L. (2016). DREADDs for Neuroscientists. *Neuron*, *89*(4), Article 4. https://doi.org/10.1016/j.neuron.2016.01.040

Schmidt, R. A., & Lee, T. D. (2019). *Motor Learning and Performance: From Principles to Application*. Human Kinetics.

Shadmehr, R., & Wise, S. P. (2004). *The Computational Neurobiology of Reaching and Pointing: A Foundation for Motor Learning*. MIT Press.

Singer, M. L., Rana, S., Benevides, E. S., Barral, B. E., Byrne, B. J., & Fuller, D. D. (2022). Chemogenetic activation of hypoglossal motoneurons in a mouse model of Pompe disease. *Journal of Neurophysiology*, *128*(5), 1133–1142. https://doi.org/10.1152/jn.00026.2022

Smith, M. A., & Shadmehr, R. (2005). Intact Ability to Learn Internal Models of Arm Dynamics in Huntington's Disease But Not Cerebellar Degeneration. *Journal of Neurophysiology*, *93*(5), Article 5. https://doi.org/10.1152/jn.00943.2004

Synofzik, M., Lindner, A., & Thier, P. (2008). The Cerebellum Updates Predictions about the Visual Consequences of One's Behavior. *Current Biology*, *18*(11), Article 11. https://doi.org/10.1016/j.cub.2008.04.071

Takeoka, A., Vollenweider, I., Courtine, G., & Arber, S. (2014). Muscle Spindle Feedback Directs Locomotor Recovery and Circuit Reorganization after Spinal Cord Injury. *Cell*, *159*(7), Article 7. https://doi.org/10.1016/j.cell.2014.11.019

Talpalar, A. E., Bouvier, J., Borgius, L., Fortin, G., Pierani, A., & Kiehn, O. (2013). Dual-mode operation of neuronal networks involved in left–right alternation. *Nature*, *500*(7460), 85–88. https://doi.org/10.1038/nature12286

Taylor, J. A., Klemfuss, N. M., & Ivry, R. B. (2010). An Explicit Strategy Prevails When the Cerebellum Fails to Compute Movement Errors. *The Cerebellum*, *9*(4), Article 4. https://doi.org/10.1007/s12311-010-0201-x

Todd, A. J. (2010). Neuronal circuitry for pain processing in the dorsal horn. *Nature Reviews. Neuroscience*, *11*(12), Article 12. https://doi.org/10.1038/nrn2947

Todd, A. J. (2017). Identifying functional populations among the interneurons in laminae I-III of the spinal dorsal horn. *Molecular Pain*, *13*, 1744806917693003. https://doi.org/10.1177/1744806917693003

Wang, Y., Chen, Y., Chen, L., Herron, B. J., Chen, X. Y., & Wolpaw, J. R. (2024). Motor learning changes the axon initial segment of the spinal motoneuron. *The Journal of Physiology*, *602*(9), Article 9. https://doi.org/10.1113/JP283875

Wolpaw, J. R. (2007). Spinal cord plasticity in acquisition and maintenance of motor skills. *Acta Physiologica*, *189*(2), Article 2. https://doi.org/10.1111/j.1748-1716.2006.01656.x

Wolpaw, J. R. (2010). What can the spinal cord teach us about learning and memory? *The Neuroscientist: A Review Journal Bringing Neurobiology, Neurology and Psychiatry*, *16*(5), Article 5. https://doi.org/10.1177/1073858410368314

Wolpert, D. M., Miall, R. C., & Kawato, M. (1998). Internal models in the cerebellum. *Trends in Cognitive Sciences*, *2*(9), Article 9. https://doi.org/10.1016/S1364-6613(98)01221-2

Xu, Y., Lopes, C., Qian, Y., Liu, Y., Cheng, L., Goulding, M., Turner, E. E., Lima, D., & Ma, Q. (2008). Tlx1 and Tlx3 Coordinate Specification of Dorsal Horn Pain-Modulatory Peptidergic Neurons. *The Journal of Neuroscience*, *28*(15), Article 15. https://doi.org/10.1523/JNEUROSCI.4126-07.2008

Yakovleff, A., Roby-Brami, A., Guezard, B., Mansour, H., Bussel, B., & Privat, A. (1989). Locomotion in rats transplanted with noradrenergic neurons. *Brain Research Bulletin*, *22*(1), 115–121. https://doi.org/10.1016/0361-9230(89)90135-4

Zhang, J., Lanuza, G. M., Britz, O., Wang, Z., Siembab, V. C., Zhang, Y., Velasquez, T., Alvarez, F. J., Frank, E., & Goulding, M. (2014). V1 and V2b Interneurons Secure the Alternating Flexor-Extensor Motor Activity Mice Require for Limbed Locomotion. *Neuron*, *82*(1), 138–150. https://doi.org/10.1016/j.neuron.2014.02.013